

S T A T U S R E P O R T

TO THE

CORROSION CONTROL
PROJECT ADVISORY COMMITTEE

March 23, 1995

Corrosion Control Annual Research Review

March 23, 1995

Institute of Paper Science and Technology

500 10th Street, NW

Atlanta, GA 30318

TABLE OF CONTENTS

LIST OF TABLES	iii
----------------------	-----

TABLE OF FIGURES	iv
------------------------	----

PROJECT F018

RECOVERY BOILER CORROSION	1
---------------------------------	---

TECHNICAL REVIEW	3
------------------------	---

INTRODUCTION	5
--------------------	---

Summary of Key FY 93-94 Results	7
---------------------------------------	---

Gas Phase Tests	7
-----------------------	---

Local Measurement of Sulfur and Oxygen Activity	8
---	---

Long-term Kinetics	8
--------------------------	---

Port Corrosion	9
----------------------	---

DISCUSSION OF FY 94-95 RESULTS	11
--------------------------------------	----

Task 1: GAS PHASE REACTIONS	13
-----------------------------------	----

IPST-funded Effect of SO ₂ on the Corrosion of Carbon Steel	13
--	----

TASK 2: LOCAL MEASUREMENT OF ENVIRONMENT BENETH FROZEN SMELT	17
--	----

TASK 3: LONG-TERM KINETICS	19
----------------------------------	----

Experimental Procedure	19
------------------------------	----

Experimental Results and Discussion	20
---	----

TASK 4: PORT CORROSION	25
------------------------------	----

Hot Corrosion in Molten Hydroxide	25
---	----

Hot Corrosion in Molten Smelt	28
-------------------------------------	----

CONCLUSIONS	33
-------------------	----

IMPLICATIONS FOR THE INDUSTRY	35
-------------------------------------	----

MAJOR PROPOSALS SUBMITTED	37
---------------------------------	----

TABLE OF CONTENTS (continued)

PROJECT F019

CORROSION CONTROL IN CLOSED-CYCLE MILLS 39

TECHNICAL REVIEW 41

LIST OF TABLES

Table 1.	Overall Recovery Boiler Corrosion Program at IPST	11
Table 2a.	Results of Static, Cyclic and Pre-Oxidation Conditions on Corrosion of Carbon Steel at 360°C in 1% SO ₂	16
Table 2b.	Results of Static, Cyclic and Pre-Oxidation Conditions on Corrosion of Carbon Steel at 360°C in 100 ppm SO ₂	16
Table 3.	Test Comparisons at 400°C for Carbon Steel. Rates are for specific periods over the entire test	21

TABLE OF FIGURES

Figure 1.	Schematic of the Experimental Arrangement	43
Figure 2.	Schematic of Furnace Details	45
Figure 3.	Corrosion Rate for Carbon Steel at 360°C under Constant Environmental Conditions	47
Figure 4.	Corrosion Rates for Carbon Steel at 360°C Under Cyclic Environmental Conditions	49
Figure 5.	Results Showing Preoxidation of Carbon Steel in 100 ppm SO ₂ at 360°C does not Stop Acceleration of Corrosion	51
Figure 6.	Schematic of the Quartz Spring Balance	53
Figure 7.	Weight Gain vs. Time for Cyclic Tests of Carbon Steel at 400°C	55
Figure 8.	Weight Gain vs. Time for Carbon Steel in 1% H ₂ S at 400°C	57
Figure 9.	Weight Gain vs. Time for Carbon Steel in 1% SO ₂ of 400°C	59
Figure 10.	Comparison of Curves from Figures 7, 8, and 9	61
Figure 11.	Experimental Set Up for Basicity and Solubility Measurements in Molten Hydroxide	63
Figure 12.	Phase Stabilities in Na-Cr-O-H System at 350°C. Three experimental basicities are Shown on the Diagram	65

TABLE OF FIGURES (continued)

Figure 13. Cr Concentration vs. Time for Different Basicities	67
Figure 14. Current vs. Time for Carbon Steel Coupled to Stainless Steel in Molten Smelt at 800°C	69
Figure 15. Photograph of the Carbon Steel and Stainless Steel wire Samples at the end of the Galvanic Test	71
Figure 16. Current vs. Time Curve for Galvanic Measurements	73
Figure 17. Carbon Steel Corrosion products after Corrosion in Molten Smelt at 800°C. Uncoupled	75
Figure 18. Current vs. Time Curve for Galvanic Measurements	77
Figure 19. Stainless Steel Corrosion Products after Corrosion in Molten Smelt at 800°C. Uncoupled	79

**RECOVERY BOILER CORROSION
PROJECT F018**

ANNUAL RESEARCH REVIEW

March 23, 1995

Jeffery A. Colwell

Gregory J. Fonder

Institute of Paper Science and Technology

500 10th Street, NW

Atlanta, GA 30318

TECHNICAL PROGRAM REVIEW

Project Title: RECOVERY BOILER CORROSION
Project Code: CORRN
Project Number: 3628/F018
Division: Chemical and Biological Sciences
Project Staff: J. Colwell, G. Fonder
FY 94-95 Budget: \$128,000

Program Objective:

Improve safety and increase operating life of equipment by proper selection of construction materials and by identifying suitable process conditions.

Summary of Results:

The cyclic oxidation/sulfidation tests were conducted using lower concentrations of SO₂. The accelerating effect was still observed as the stable product scale cycled from sulfide to oxide. Thermodynamic calculations indicate that for typical black liquor compositions, both 100 ppm and 1% concentrations of SO₂ are possible as a reaction product in boilers. To help understand these observations, a proposal for detailed metallographic scale analysis is being submitted to Oak Ridge National Laboratory. This will be done in the HTML User Facility, and a response should be available sometime after June. There will be no costs associated with the analysis provided the results can be published jointly by IPST and ORNL.

The effect of small alloy additions to carbon steel is currently being investigated by exposing T-22 to typical lower furnace atmospheres. The data will be compared with the existing IPST database for plain carbon steel, and the initial results should be available by late March.

The quartz spring balance results show that repeated tests produce corrosion rates that are within about a factor of 2 for certain segments of the exposure. The breakaway points do vary, which has not been quantified as yet. However, a scale thickness of about 160 microns did cause a spallation event in one case, and we suspect that this may be a critical thickness which might indicate when rapid sulfidation will begin. Tests in this apparatus also showed how a test in SO₂ produced parabolic-type kinetics (rate decreasing with time), and in H₂S, kinetics remained parabolic because of scale spallation. Of more concern was the altering sulfidation/oxidation experiment, because

the *instantaneous rate* increased with time, looking more like an exponential function. This has serious implications for operations.

The experiments of Ph.D. candidate Matt Estes are continuing. Solubility measurements are being made as a function of melt basicity in molten hydroxide. The shape of the curves are beginning to look like the corrosion rate versus basicity curves presented previously. More data are expected to be available for the paper to be presented at the next TAPPI Engineering Conference.

Corrosion tests in molten smelt were conducted to answer some of the PAC's questions. We found that carbon steel and stainless steel corroded at very fast rates: on the order of several thousand mpy. Galvanic corrosion measurements indicate that there is a galvanic effect, but it is a minor contribution that only amounts to tens of mpy rather than the baseline corrosion rate in the thousands. Consequently, we are of the opinion that air port corrosion is a result of hot corrosion in hydroxide based salts.

Biochem Corrosion (Colwell):

Goals for 1995-1996:

Experiments will continue on alloys with small additions of scale-forming elements. The objective will be to try to determine what components and concentrations in an alloy are necessary for recovery boiler service. This would have economic impact on the cost of tubes and may also point the way for coating development. Cyclic oxidation/sulfidation experiments are showing how scale growth kinetics are impacted by instantaneous changes, so this work will continue. Moreover, the molten smelt testing procedures which have been developed here will be of use in the ORNL funded project on composite tube cracking. It is proposed that the molten smelt work continue with various smelt additives to reduce the melting point and to investigate further the effect of the cover gas. It is our hypothesis that this is also a hot corrosion mechanism and melt basicity (acid gas content) will play a role in the observed corrosion rates.

INTRODUCTION

The main objective of this project is to understand the causes of corrosion on the waterwall tubes in the lower furnace of the kraft recovery boiler. Once those causes are better understood, it is expected that mitigation strategies can be developed which will have a sound basis. Problems on the fireside and coldside have been observed by many mills, and corrosion has been implicated in several smelt-water explosions over the years. Obviously, safe operation of the boiler is of prime concern, so IPST has been aggressively pursuing research which will contribute to the general, and specific, understanding of recovery boiler corrosion.

The focus of this program is consistent with IPST's goals for its dues-funded research program in that it is longer term with an emphasis on a fundamental understanding rather than a short term quick fix without any understanding of the underlying reasons for the observed behavior. This program is also being leveraged with Ph.D. student research, with a budget independent of this particular dues-funded project, as well as externally funded projects.

SUMMARY OF KEY FY 93-94 RESULTS

The work completed during the previous fiscal year was designed to increase our understanding of corrosion in kraft recovery boilers. It is our belief that increasing our understanding can ultimately be used to help extend the operating life of boilers by minimizing corrosion. There have historically been four main objectives of this project, with each treated as a separate project task.

Some of the more interesting past results are reviewed here to provide a point of reference for the discussion of more recent results obtained this fiscal year.

Gas Phase Tests

The AFPA-funded Phase D work was completed and very nicely extended the gas matrix work previously conducted by IPST. A series of twenty experiments was conducted to study corrosion in the lower furnace using a standard test developed at PPRIC. The experiments were designed to investigate SA-210 carbon steel and AISI Type 304 stainless steel in a variety of temperature and gaseous environments. The matrix was designed to determine the sensitivity of corrosion to several parameters which would be expected to vary in operating boilers. Additional tests were conducted by PPRIC using the same test procedure and metal coupons machined from the same tube samples. Several interesting results were seen in the experimental data. The effect of thermal cycling in an H₂S only environment had a threshold number of cycles above which the corrosion rate increases rapidly. This same threshold was not seen in more complex environments, or, it could be that the threshold in these cases is less than the minimum number (10) of cycles used. The addition of hydrogen to the gas mixture caused an increase in the corrosion rate at the same sulfur partial pressure (assuming that equilibrium is reached). A possible explanation, based on defect concentrations in the

scale, was discussed in last year's report. Also noted was the fact that methyl mercaptan was much more aggressive toward carbon steel than stainless steel.

Work on the effect of SO_2 on the corrosion of carbon steel was emphasized once the AFPA work was completed and more furnace space became available. Thermodynamic calculations revealed that unless some H_2S is present, iron oxides are more stable than iron sulfides. Because there is more interest in conditions where iron sulfide is stable, the use of simple gases containing only SO_2 was not pursued.

However, based on the thermodynamic calculations, experiments were conducted which had cyclic coupon exposures to oxidizing and sulfidizing environments. The corrosion rates measured under various conditions are summarized in Table 2a. The most important conclusion drawn from this data is that if a boiler tube is exposed to conditions that change from stable sulfide products to stable oxide products, corrosion can be expected to accelerate.

Local Measurement of Sulfur and Oxygen Activity

Efforts on this task were postponed during the fiscal year for two reasons. First, a proposal to DOE on developing sensors for boilers, which is also the next phase of the AF&PA recovery boiler corrosion project, was issued. And, second, with the limited staff available for this overall project, the resources were allocated to other tasks.

Long-term Kinetics

A quartz spring balance was constructed to conduct the long-term trials. The first test was conducted in a 1% H_2S , 5% H_2O environment. The balance is only able to record changes in overall weight based upon the growth or spalling of scale on the test sample. Therefore, an empirical value based upon weight loss to weight gain ratios observed for

similar environments in the past of between 2.0 and 2.25 is used to convert from weight gain to weight loss. Weight loss or metal recession is the measurement of most interest because the remaining metal thickness will control the life of the component. The corrosion kinetics appeared to be linear, after an initial period of apparent weight loss (due to mechanical properties of spring), with a rate of 250-280 mpy.

Port Corrosion

The IPST field probe, discussed and described in previous reports, was installed in a Mead boiler to collect deposits and measure the melting point. The probe is designed to allow the *in situ* measurement of deposit melting temperatures because after the deposits are removed from boilers the melting temperature is likely to change as the composition of the deposit changes as a result of reactions with air.

The actual melting point determination was performed by Mead personnel with a resulting value of 540°F. The previous value found in a Stone boiler was 562°F, which is remarkably similar. Chemical analysis of the deposit after removal from the boiler reveals that it is mostly Na_2CO_3 and Na_2SO_4 . This is not unexpected since any NaOH actually present on the probe when the measurements were being made would have been converted to Na_2CO_3 upon reaction with the CO_2 present in air after the removal from the boiler. The measured melting point was very close to the published eutectic temperature for the NaOH- Na_2CO_3 system.

A Ph.D. student (Matt Estes) undertook the task of making oxide solubility measurements as a function of basicity to test the hot corrosion postulate for corrosion at air ports. A basicity probe utilizing β -alumina and zirconia was built and tested. β -alumina is an exclusive Na^+ conductor, and zirconia is an O^{2-} conductor, so the combination allows an indirect determination of Na_2O activity to be measured based upon the equation

$$E = E^{\circ} - \frac{RT}{2F} \ln a_{Na_2O} + \frac{RT}{4F} \ln P_{O_2}$$

The range of basicity available for experiments appears to be about 4 orders of magnitude. Other details regarding how to optimize the probe behavior were also completed.

DISCUSSION OF FY 94-95 RESULTS

This project has been divided into several different tasks to focus our efforts on areas that need the most attention. Table 1 gives an overview of the structure of the overall program and shows how it is leveraged with other related activities, such as student research and research funded by others. Next to each task is a brief description of the main objective or the question which needs to be answered.

Table 1. Overall Recovery Boiler Corrosion Program at IPST

<i>Dues-Funded (F018)</i>	<i>Additional Funding Leverage</i>
Task 1. Gas Phase Reactions Determine Suitable C,O,S Potentials	AF&PA Phases C&D
Task 2. Local Measurements Develop Sensor for O and S Beneath Frozen Smelt	DOE/AF&PA Corrosivity Monitoring (?)
Task 3. Long-term Kinetics Extrapolation of Lab Tests to Predict Service Performance	
Task 4. Port Corrosion Determine Mechanism to Develop Efficient Mitigation Strategy	Ph.D. Student Estes
	ORNL/DOE Composite Tube Cracking

The remainder to the report is organized to cover the status of each of the tasks shown in Table 1. The objectives of the composite tube cracking project are covered last; the project has only recently begun.

TASK 1: GAS PHASE REACTIONS

The premise of this task is that corrosion of waterwall tubes is a result of a reaction with gases which cause oxides and sulfides to form. If only iron oxides are formed, then the corrosion is minimal, but when iron sulfides form, the kinetics are rapid which consumes the base metal at a rate much faster than can be tolerated. The presence of a frozen smelt layer does not directly cause corrosion, but reactions between it and gases which pass through the layer can react to form an environment beneath the smelt which is very different than the bulk gas in the furnace. As a result, the micro-environment beneath the smelt will control corrosion kinetics and tests which simulate that environment would be the best to understand the corrosion mechanism. The IPST environments were selected in order to meet several objectives; employing components representative of the furnace environment, using mixtures which will accelerate the corrosion rate but still give similar scales, and using temperatures that are likely to be encountered under the frozen smelt layer.

IPST-funded Effect of SO₂ on the Corrosion of Carbon Steel

As mentioned in the summary of last year's work on this topic, the effect of SO₂ on the corrosion rate of carbon steel was investigated using an SO₂ level of 1%. Further work in this fiscal year was done using an SO₂ level of 100 ppm. Both levels are within the range of values calculated using HSC Chemistry for Windows[®] based on typical black liquor compositions, and assumes that equilibrium is attained. While the extent of that approach to equilibrium is unknown, for these tests it is important to establish equilibrium so that good repeatability can be maintained. The experimental procedures used are the same as those reported in our previous work.

Single-zone vertical tube furnaces are used for all tests. A 2.5 inch diameter Vycor or AV-30 tube is used as the test chamber. The test gas is introduced at the bottom of the

chamber and exhausted from the top and passed through a caustic gas scrubber. A Pyrex coupon holder attached by a flexible chain to a short piece of Pyrex rod is used to position the coupons in the center of the constant temperature zone of the furnace. The gas mixture entering the chamber is set using mass flow controllers. Schematic drawings of the furnace and plumbing arrangements are shown in Figures 1 and 2.

Prior to each test, the furnace temperature is raised to 800°C, held there for several hours, and then allowed to cool to 100°C. The reason for this procedure is to ensure that any sulfur deposits are burned off so that they do not influence subsequent tests which may use a lower sulfur partial pressure. After this initial soak, the following procedure is followed to ensure consistent results:

1. remove 6 coupons from desiccator and clean with acetone
2. weigh and record coupon ID, weight, and surface area
3. remove upper flange plate from furnace tube
4. attach coupons to specimen holder using platinum wire
5. insert coupon holder assembly into upper flange plate
6. attach upper flange plate to furnace tube
7. purge tube with N₂ for 10-15 minutes
8. raise furnace temperature to operating value while maintaining N₂ purge
9. turn off N₂ purge when operating temperature is reached
10. adjust gas mixture flow rates to the desired level
11. record start time of test

During the course of a test the operating parameters are monitored and adjusted if necessary. A consistent procedure is also followed at the conclusion of every test. The test gas mixture is turned off and a N₂ purge is initiated. The furnace is allowed to cool to room temperature before the coupons are removed. The coupons are then carefully

removed from the furnace and visually inspected. Of the six coupons removed, four are used for weight loss determination, one for mounting and subsequent metallographic examination, and one stored “as is” as an archival specimen. The coupons used for weight loss determination are cleaned by blasting with glass beads and rinsing with acetone. Calibration coupons have been tested to ensure that significant base metal is not removed during glass bead blasting.

The results of the 100 ppm SO₂ tests are listed in Table 2 along with the the corresponding 1% SO₂ tests. The results are further conveniently grouped into three distinct classes as shown in Figures 3-5. For comparison with the 1% SO₂ tests, several of these results are included in the figures. Figure 3 shows what happens when SO₂ is added to H₂S. Even small amounts cause the rate to increase, which is related to the approach of the sulfide/oxide boundary, because the sulfur partial pressure is essentially constant. In Figure 4, cycling can be seen to accelerate when the environment is cycled between oxidizing and sulfidizing conditions. While the 100 ppm SO₂ case is not as dramatic as the 1% SO₂ tests, it does show that the rate is higher than the average of the two different environmental conditions. We suspect that the rate of conversion of oxide scales to sulfide scales and back plays a role here. So, the length of each segment of the cycle will also play a role as will the “strength” of the oxidizing or sulfidizing conditions.

To test this, preoxidation tests were conducted to determine whether scale breakdown events could be quantified. Preoxidation in 100 ppm SO₂ was conducted for 3 days, followed by sulfidation at various times. As can be seen, just 7 hours in H₂S is sufficient to convert the scale and accelerate the corrosion kinetics. So, short-term changes in the boiler would also be sufficient to cause rapid attack in certain locations.

Table 2a. Results of Static, Cyclic and Pre-Oxidation Conditions on Corrosion of Carbon Steel at 360°C in 1% SO₂

<i>Environment</i>	<i>Test Duration</i>	<i>Corrosion Rate (mpy)</i>
1% H ₂ S	5 days	5.1
1% SO ₂	5 days	2.9
0.5% H ₂ S + 0.5% SO ₂	5 days	8.7
1% H ₂ S ↔ 1% SO ₂	1 day each for 5 days	21
1% SO ₂ ↔ 0.5% SO ₂ , 0.5% H ₂ S	1 day each for 5 days	10.6
0.5% SO ₂ , 0.5% H ₂ S ↔ 1% SO ₂	1 day each for 5 days	11.7
1% SO ₂ → 1% H ₂ S	3 day SO ₂ , 1 day H ₂ S	11.2
1% SO ₂ → 1% H ₂ S	3 day SO ₂ , 7 hours H ₂ S	11.9
1% SO ₂ → 1% H ₂ S	3 day SO ₂ , 16 hours H ₂ S	16.6

Table 2b. Results of Static, Cyclic and Pre-Oxidation Conditions on Corrosion of Carbon Steel at 360°C in 100 ppm SO₂

<i>Environment</i>	<i>Test Duration</i>	<i>Corrosion Rate (mpy)</i>
1% H ₂ S	5 days	5.1
100 ppm SO ₂	5 days	2.1
0.5% H ₂ S + 50 ppm SO ₂	5 days	5.5
100 ppm SO ₂ ↔ 1% H ₂ S	1 day each for 5 days	6.6
1% H ₂ S ↔ 100 ppm SO ₂	1 day each for 5 days	4.8
100 ppm SO ₂ → 1% H ₂ S	3 days SO ₂ , 7 hours H ₂ S	8.6
100 ppm SO ₂ → 1% H ₂ S	3 days SO ₂ , 16 hours H ₂ S	8.7
100 ppm SO ₂ → 1% H ₂ S	3 days SO ₂ , 1 day H ₂ S	10.3

TASK 2: LOCAL MEASUREMENT OF ENVIRONMENT

BENEATH FROZEN SMELT

The local thermodynamic conditions beneath a frozen smelt layer will obviously control the kinetics of scale growth more than the bulk gas chemistry in the furnace. While it may be possible to develop models to predict these conditions, it is always better if a direct measurement can be made.

The objective of this task is to develop a technique based on solid electrolytes. Solid electrolytes are typically exclusive ionic conductors which can be used to measure a thermodynamic quantity, relative to the conducting species, on one side of the electrolyte if the value on the other side is known. Thus if the value is fixed in an experiment, the device becomes a probe capable of determining instantaneous values for the thermodynamic potential of interest. For this case, we are primarily interested in knowing what the local sulfur and oxygen activities are beneath the smelt, because these conditions will control sulfidation and oxidation kinetics.

Efforts on this task were postponed during this fiscal year for two reasons. First, a proposal to DOE on developing a corrosivity monitor for boilers has been issued. It is our understanding that the proposal has a good chance for funding and is slated for additional cost sharing by AF&PA as part of their recovery boiler corrosion program. And second, with the limited staff available for this overall project, the resources were allocated to other tasks, which is consistent with previous PAC discussions.

TASK 3: LONG-TERM KINETICS

Boilers are designed to operate for many thousands of hours without replacing waterwall tubes. Even between scheduled shut-downs the boiler must operate for 4,000 to 8,000 hours, depending upon individual mill maintenance plans. Most of IPST's laboratory tests are at most a few hundred hours and usually much less than that. Alloy rankings are made based on these short-term experiments as is an estimate of remaining alloy life. An implicit assumption in this approach is that the kinetics do not change and the rate laws developed are constant. This has not been demonstrated for this application, and the data generated by discrete weight change measurements show gaps which need to be better defined if accurate kinetic rate laws are a desired result. In other industries, a phenomenon known as breakaway corrosion has been reported for stainless steels. Breakaway corrosion occurs as a result of depletion of the scale-forming element and causes the kinetics to change from parabolic to linear with a higher corrosion rate. This task is designed to determine whether this phenomenon is likely to occur in the recovery boiler environment by making continuous measurements of the weight change.

Experimental Procedure

As was discussed previously, the gravimetric apparatus has been redesigned to prevent the buildup of sulfur condensation on the sample hangdown wire. To accomplish this, the temperature from the sample to the quartz spring (material which can withstand the resulting temperature without deleterious effects) must be maintained above the melting point of sulfur. This was done by wrapping the upper portion of the furnace tube with high-temperature heating tape. A schematic of the experimental arrangement is shown in Figure 6.

Prior to each test with a different gas mixture, the furnace is burned out to remove deposits, as was explained under Task 1. A coupon of known surface area is cleaned with

acetone and weighed. All coupons are previously prepared using the procedures that have already been discussed. The coupon is attached to the platinum hangdown chain and then carefully placed into the furnace. The furnace temperature is then slowly raised to the test temperature under a N_2 atmosphere. The coupon is allowed to stay under this atmosphere for a short time to allow the quartz spring to come to equilibrium. The flow of test gases is then started. The weight is monitored visually using a cathetometer by measuring the change in spring extension as a function of time. This can be done using Hooke's law because the spring constant is known.

Experimental Results and Discussion

A summary of the data collected using the quartz spring balance apparatus is provided in Table 3.

The first six tests were conducted using the same gaseous environment to check for repeatability. The curves vary, with transitions in corrosion rates at different times. This shows the variability in scaling kinetics which can be observed in nominally the same tests. The first test gives a corrosion rate that is 50 % higher than previous trials conducted using discrete weight loss experiments (175 mpy) in the same environment. Given that this was the first test, perhaps it can be discounted on that basis alone.

The second test starts at a lower rate, 60 to 70 mpy, with the second half of the test giving a result, 160 to 175 mpy, that agrees well with the discrete specimen results. The next four tests all produced corrosion rates from 30 to 80 mpy over different time periods. So, neglecting the second segment in Test 2, the rates for these tests are within a factor of about 2. In Test 2, there was an obvious acceleration of the slope of the curve, but at this point we do not know what triggered it.

Table 3. Test Comparisons at 400° C for Carbon Steel. Rates are for specific time periods over the entire test.

<i>Test</i>	<i>Environment</i>	<i>Time (hour)</i>	<i>Corrosion Rate (mpy)</i>
1	1% H ₂ S, 5% H ₂ O, balance N ₂	75-350	250-280
2	1% H ₂ S, 5% H ₂ O, balance N ₂	10-200	60-70
	1% H ₂ S, 5% H ₂ O, balance N ₂	200-500	160-175
3	1% H ₂ S, 5% H ₂ O, balance N ₂	70-500	35-40
4	1% H ₂ S, 5% H ₂ O, balance N ₂	70-500	75-85
5	1% H ₂ S, 5% H ₂ O, balance N ₂	6-100	47-53
6	1% H ₂ S, 5% H ₂ O, balance N ₂	80-1000	32-37
7	1% SO ₂ , balance N ₂	40-160	16-20
	1% H ₂ S, balance N ₂	190-330	35-40
	1% SO ₂ , balance N ₂	335-430	30-35
	1% H ₂ S, balance N ₂	435-595	60-70
	1% SO ₂ , balance N ₂	600-760	60-70
	1% H ₂ S, balance N ₂	770-950	45-55
	1% SO ₂ , balance N ₂	960-1050	45-55
8	1% H ₂ S, balance N ₂	25-600	45-55
	1% H ₂ S, balance N ₂	770-1020	36-44
9	1% SO ₂ , balance N ₂	30-850	50-55
	1% SO ₂ , balance N ₂	860-1000	28-32

The seventh test was performed using alternating H₂S/N₂ and SO₂/N₂ mixtures in order to see the effect of changing environment on corrosion rate. We had done similar tests, reported previously in Task 1, which showed a greatly accelerated corrosion rate as a result of changing from oxidizing to sulfidizing conditions and back. So, we used this apparatus to determine what the instantaneous kinetics were as the environment was changed in a similar way. Because the other test method only allows the collection of a single data point, the objective of this experiment was to determine how the accelerating

change occurred as it was happening. The data show two important aspects; one, the rate during subsequent segments of the same environment tends to increase, and two, there is an “offset” with a very high initial rate during the early stages of environmental change within each segment. This data is also graphically depicted in Figure 7. This graph might be considered somewhat misleading because the weight loss to weight gain ratios are different for the oxide and sulfide segments, with the oxide having a larger value. Of course, this is under the assumption that the scales are completely altered fairly rapidly, and this seems to be true if the initial high weight change at the beginning of each cycle is a result of this conversion. The eighth and ninth tests are baselines for the cyclic test (Test 7), which were allowed to run out for 1000 hours to give comparisons for the same time period and are also given in Figures 8 and 9.

A comparison of the last three tests is given in Figure 10. The most important thing to notice is the slopes and the curvatures of these graphs. There is very much similarity between the baseline runs with the 1% H₂S and 1% SO₂ over the first 600 hours. At 600 hours the sulfide scale appears to have spalled. The weight of the sample recovered over 200 additional hours, which is consistent with the extent of weight gain found for the first 200 hours of exposure. Note that the SO₂ curve shows an ever decreasing slope over the last several hundred hours. This is indicative of parabolic kinetics and would be expected of an oxide scale layer which is protective. This is in contrast with the last 200 hours of the sulfide scale which shows the rate continues at a rate that is just slightly lower than the initial segment. We believe that had the test run a little longer, the slope would have been very close to the initial sulfidizing segment as the kinetics reached steady state.

Apparently, at 600 hours under these conditions, the sulfide scale reached a limiting thickness of approximately 160 microns which caused a spallation event. This may be an important result in that we this may define a condition which would indicate when rapid

sulfidation corrosion begins. Of course, substrate curvature will influence this in practice, but any temperature and environment combination which would give that scale thickness could be used to estimate when spallation would be observed.

Another interesting point from Figure 10 is that the cyclic test shows the opposite curvature from the oxidation and sulfidation runs. This is very worrisome because it indicates an ever-increasing corrosion rate with time. While the later stages indicate that the rate may be leveling off, if the scale spalls, the kinetics begin again at the initial rate, and acceleration of corrosion would continue. These experiments may have quantitatively shown the severity of local environment changes on corrosion and the importance of understanding the details of the corrosion reactions before realistic mitigation strategies can be implemented.

TASK 4: PORT CORROSION

Because of excessive fireside sulfidation corrosion of carbon steel waterwall tubes boiler manufacturers began offering composite tubes for lower furnace applications. Composite tubes are manufactured with a carbon steel inner tube for corrosion prevention on the waterside and a stainless steel outer tube which protects against fireside corrosion. This combination has provided a good compromise in performance and has allowed boilers to be operated at higher pressures.

As boiler operating pressures continued to rise, a problem of corrosion at air ports has been occasionally observed. This has also been seen at other ports. Corrosion of the stainless steel outer layer occurs very rapidly until it is completely consumed. Then, when the underlying carbon steel is exposed, the corrosion of the tubes slows considerably and is minimal thereafter. Because the stainless steel was used to prevent corrosion of the carbon steel tubes, there is obvious concern when the carbon steel is exposed. Many researchers, including IPST, believe that the cause of this attack is due to the presence of molten NaOH-based salts in stagnant flow areas. While some sulfur will undoubtedly be present in the salt, it is essentially hydroxide. The NaOH mechanism is not universally accepted, however. The mechanism for this attack is under investigation because the industry needs to know how to prevent it. There have not been any tube ruptures so far, but the severity of the corrosion justifies our work to solve the problem.

Hot Corrosion in Molten Hydroxide

This work has been undertaken by Matt Estes to fulfill part of his Ph.D. degree requirements. The theoretical model has been previously presented here and elsewhere, so will not be repeated. However, one of the key elements is that the solubility of various oxides on the surface of alloys in the salt will control the dissolution of the alloy. The

solubility will be a function of salt basicity, so corrosion will also be a function of salt basicity.

Currently there are three furnaces available for data collection, but shortly two additional set-ups will also be available. The tests take some time for equilibrium to be attained, so the multiple set-ups will allow more data to be taken in a reasonable time period. Figure 11 shows the experimental arrangement. Salt samples are taken for subsequent solubility measurements by using a ceramic rod placed through a port opening. The depth of the rod insertion has been calibrated so that a sample of approximately 1 cm is taken. The sample freezes in about 2 seconds, and then it is removed for analysis.

A computer with an analog input card that has 8 channels capable of measuring both temperature and voltage has been installed. The computer will make monitoring of the basicity of the melt and the temperature much easier. Because of the 8 channel limitation, two furnaces will not have detailed temperature records. But, because the furnaces have been running at a constant temperature over the last year, manual recording should be sufficient.

Experiments were completed at three different basicity ($\log a_{\text{Na}_2\text{O}}$) conditions. The basicity values are -9, -6.1, and -4 respectively for acidic, neutral, and basic. The neutral condition is achieved by flowing dry nitrogen gas over the melt. The acidic condition is achieved by adding water vapor and the basic condition is achieved by adding disodium peroxide to the melt. Variations in the extent of water vapor or disodium peroxide additions will allow the basicity to be fine tuned to the desired value.

In Figure 12, a thermodynamic phase stability diagram has been constructed for chromium in sodium hydroxide at 350°C. The black squares on the diagram represent the

locations and the conditions of the experiments. The acidic condition is very near the maximum possible value. The neutral condition is very near the chromium oxide - disodium chromate boundary, which is shown for pure compounds. Most likely there is some disodium chromate present at the neutral condition. Finally, the basic condition is in a region where disodium chromate is the thermodynamically stable compound.

The results of the solubility measurements from six runs are provided in Figure 13. The general shape of the curves is parabolic, with a rapid increase at first and leveling off as the concentration of undissolved chromium is used up. The shape of the curve indicates that the dissolving of chromium into the molten sodium hydroxide is a first order kinetic reaction. We are confident that under the neutral condition, saturation has occurred, and the measured solubility may be close to a minimum. However, for the acidic and basic conditions, it is suspected that the melt did not have enough starting material, so saturation did not occur. The peaks at short times are indicative of this. So, tests will be repeated with larger amounts of starting oxide, which will allow the solubility under these conditions to be determined. These values will undoubtedly be higher than the values shown in the figure, but it is important to note that the solubility vs. basicity curve is beginning to take the same shape as the corrosion rate versus basicity curves we presented in previous reports.

Another observation has been made regarding a slight color difference between the samples taken under the basic and neutral conditions. Both samples are the color yellow. When compared visually next to each other, however, the sample from the basic condition is yellow with an orange coloration and the neutral condition is yellow with a green coloration. The difference in color is small, but is important. A change in color can be a result of different oxidation states of the metal ion. Both samples probably have most of the chromium in +6 state as indicated by the yellow color, but they may have

slightly different percentages of chromium in +3, and +2. Chromium in the +3 state is green, and chromium in the +2 state is red. Further work will attempt to use a TAPPI standard test method 619 cm-84 to determine the concentration of chromium in the hexavalent state.

Some experiments were also conducted to measure the solubility of iron oxide NaOH. Red iron oxide, Fe_2O_3 did not dissolve under neutral or acidic conditions. The concentration of iron under both conditions after 30 days was less than 1 part per billion (ppb) which is the maximum sensitivity of the ICP machine. However, iron oxide under the basic condition became a black solution with iron present. An experiment is currently underway to measure the solubility of iron oxide under a basic condition. Previous weight loss corrosion tests reported here showed that AISI 1010 carbon steel corroded very slowly in NaOH. Perhaps the formation of Fe_3O_4 is the controlling step in basic solutions. Future tests using Fe_3O_4 will be tried under the different basicity conditions to determine the effect of the oxide present on the surface of the steel.

Hot Corrosion in Molten Smelt

An alternative to the molten NaOH hypothesis was also tested here because of the recent work presented by Westvaco, and because of the PAC's recommendations. This alternative hypothesizes that hot, molten smelt is the cause of the port corrosion seen. This is based upon the measurement of several large temperature excursions in the affected areas of some air ports. To satisfy the concerns caused by this observation, several simultaneous galvanic current and weight loss tests were conducted here. The troubling part of this proposed mechanism is that we would expect that molten smelt that could corrode stainless steel in a short period of time should also corrode carbon steel very quickly. This has not been observed in practice, and the carbon steel corrodes at a

rate much slower than stainless steel. Thus, the hot corrosion mechanism based on NaOH based salts seems to fit the observations more closely.

The first test was made using a alumina crucible containing 20 gm of artificial smelt (80% Na_2CO_3 , 12% Na_2SO_4 , 8% Na_2S) placed in an existing stainless steel retort. Due to an inability to remove the crucible from the retort at the conclusion of the test, a new test furnace was constructed and a ceramic tube was used as the retort. This change also allowed a larger (50 gm of powdered smelt) alumina crucible to be used. The galvanic current probe was built using a 4-hole ceramic tube through which two stainless steel and one carbon steel wires were fed. The fourth hole was blocked with a short piece of stainless steel wire outside the retort. The carbon steel and one of the stainless steel wires were used as working electrodes (coupled), with the remaining stainless steel wire used as a reference electrode (uncoupled). The retort was sealed with a metal cap containing ports for gas inlet and exhaust, a thermocouple, and the probe.

An initial test to determine the melting point of the smelt powder yielded a temperature of approximately 800°C. At this temperature the smelt remained molten for the duration of testing. The frozen smelt was inspected at the end of the test and appeared well mixed. For the above reasons a temperature of 800°C was used for all subsequent tests. Prior to the start of each test a new probe was built for reasons to be discussed below. To start a test the required amounts of each compound were carefully weighed out and thoroughly mixed using a mortar and pestle. Before the mixed powder was poured into the crucible, pre-weighed specimens of stainless and carbon steels were placed in the crucible for weight loss corrosion rates, with precautions to ensure that they were not touching. The desired amount of smelt powder was then poured into the crucible. The crucible was then placed in the retort and the top sealed in place. The galvanic probe is inserted into the retort just to the top of the crucible. A N_2 flow is started and the temperature slowly

raised to 800°C. The galvanic probe is then inserted into the molten smelt and the galvanic test started. The data was recorded using a Gamry CMS100 system.

As mentioned above, the first test was conducted in a small stainless steel retort. The results of the galvanic test are shown in Figure 14. There were no separate weight loss specimens used in this trial. However, several things could be seen by inspecting the electrodes of the galvanic probe. At the end of the test the stainless steel electrode was consumed and the carbon steel electrode was reduced to 20% of its initial diameter. When the ends of the probe were cleaned, it was possible to see that there was still a thin piece of stainless steel remaining. This is shown in Figure 15. The *difference* in the diameter lost between the stainless and carbon steel wires is consistent with the integrated value of the area under the current versus time curve. However, this yields a galvanic contribution to the corrosion rate which is much smaller than the total corrosion rate of either wire. The carbon steel electrode was also covered with a very thick deposit.

The first test run using the new furnace and retort design did contain weight loss specimens; the galvanic probe was inserted into the melt and the resultant curve is shown in Figure 16. The coupled stainless and carbon steel electrodes and the uncoupled stainless steel specimen, weighing 3.12 g, were completely consumed. The uncoupled carbon steel coupon appeared to be present with a very thick deposit that could not be removed by bead blasting. Further investigation revealed that, just as was the case with the carbon steel electrode, the entire piece was composed of corrosion products and was slightly magnetic (see Figure 15).

In order to see if changing the cover gas had any large affect on the galvanic current and/or weight loss tests a 1% H₂S/balance N₂ mixture was used as an initial trial. The graph of galvanic current versus time is shown in Figure 18. As was the case in the tests using a N₂ cover gas, all electrodes were missing at the end of the test. However, in this

case both weight loss coupons appeared to have remained. But, the carbon steel “coupon” was composed only of corrosion products. The stainless steel “coupon” also was only corrosion products, but unlike the homogeneous appearance of the carbon steel it was composed of three distinct parts (see Figure 19): A thin outer crystalline black layer (also present on carbon steel remnant), a black amorphous middle layer, and a gray crystalline inner core about 25% of original diameter. All three layers are fairly brittle with no discontinuities across boundaries when broken.

As can be seen from the galvanic current plots, the current begins to oscillate around zero after 24 hours. This implies that the stainless steel/carbon steel electrode pair has been consumed. Based upon the thickness of the electrode wires, this results in a calculated corrosion rate of approximately 7000 mpy for at least one of the electrodes. This is consistent with the values calculated from the uncoupled pair of stainless steel and carbon steel weight loss coupons, 9000 mpy and 3000 mpy, respectively. The numbers for the uncoupled pair are minimums because they are based on the assumption that the coupons lasted the entire duration of the tests. These values can be compared with the galvanic current corrosion rate of 40 mpy calculated from the initial test above.

CONCLUSIONS

1. The cyclic oxidation/sulfidation tests were conducted using lower concentrations of SO_2 . The accelerating effect was still observed as the stable product scale cycled from sulfide to oxide. Thermodynamic calculations indicate that for typical black liquor compositions, both 100 ppm and 1% concentrations of SO_2 are possible as a reaction product in boilers.
2. To help understand these observations, a proposal for detailed metallographic scale analysis is being submitted to Oak Ridge National Laboratory. This will be done in the HTML User Facility, and a response should be available sometime after June. There will be no costs associated with the analysis provided the results can be published jointly by IPST and ORNL.
3. The effect of small alloy additions to carbon steel is currently being investigated by exposing T-22 to typical lower furnace atmospheres. The data will be compared with the existing IPST database for plain carbon steel, and the initial results should be available by late March.
4. The quartz spring balance results show that repeated tests produce corrosion rates that are within about a factor of 2 for certain segments of the exposure. The breakaway points do vary, which has not been quantified as yet. However, a scale thickness of about 160 microns did cause a spallation event in one case, and we suspect that this may be a critical thickness which might indicate when rapid sulfidation will begin.
5. The quartz spring balance showed how a test in SO_2 produced parabolic-type kinetics (rate decreasing with time), and in H_2S , kinetics remained parilinear because of scale

spallation. Of more concern was the alternating sulfidation/oxidation experiment, because the *instantaneous rate* increased with time, looking more like an exponential function. This has serious implications for operations.

6. The experiments of Ph.D. candidate Matt Estes are continuing. Solubility measurements are being made as a function of melt basicity in molten hydroxide. The shape of the curves are beginning to look like the corrosion rate versus basicity curves presented previously. More data are expected to be available for the paper to be presented at the next TAPPI Engineering Conference.

7. Corrosion tests in molten smelt were conducted to answer the PAC's questions. We found that carbon steel and stainless steel corroded at very fast rates: on the order of several thousand mpy. Galvanic corrosion measurements indicate that there is a galvanic effect, but it is a minor contribution that only amounts to tens of mpy rather than the baseline corrosion rate in the thousands. Consequently, we still are of the opinion that air port corrosion is a result of hot corrosion in hydroxide based salts.

IMPLICATIONS FOR THE INDUSTRY

One of the most important aspect of these results is that if a boiler tube is exposed to an environment which changes the stable product phase from oxide to sulfide and back periodically, it would be expected that corrosion would be accelerated substantially. If we superimpose the result that a certain number of thermal cycles over a threshold value will also cause rapid corrosion, it is not surprising that some areas of some boilers can be subjected to severe damage. Because changes in local gas composition would be expected in the rapidly changing boiler environment, these findings may contribute to the explanation of why some boilers corrode in certain areas while others do not. It is also important to note that the impact of various environmental parameters, such as water or carbon dioxide, is to increase the corrosion rates by different degrees. Consequently, the prediction of corrosion rates at a particular location at a specific time is extremely challenging. Furthermore, we have been able to quantify how the instantaneous corrosion rate accelerates with time as a result of alternating oxidizing and reducing conditions. This is of concern because it makes long-term predictions of rates difficult and may again explain why some boilers corrode much worse than others.

Our studies of air port corrosion have shown that depending upon the basicity of the melt, a number of different alloy classes can have widely varying corrosion behaviors. Thus, the variability in reported service problems might be explained by variable basicities of the condensed salts at the ports. Our studies will be useful in describing this behavior in more detail. It is our goal that eventually the laboratory probes developed here might be used in the field to characterize melt behavior and lead us to proper alloy selection based on actual melt chemistries in specific boilers.

MAJOR PROPOSALS SUBMITTED

We have several opportunities for external funding leverage which will be summarized briefly here:

1. Corrosivity Monitoring in Kraft Recovery Boilers.

Funding from DOE is being sought to develop a device or a methodology to measure conditions which control corrosion in recovery boilers. The goal will be to get enough information in a reasonable time frame so that operating parameter changes can be made with an eye toward the impact of the decision on corrosion. The project will be conducted by IPST, Paprican, and ORNL, with significant cost sharing by AFPA. The scope of the project is consistent with the AFPA Phase E program on recovery boiler corrosion testing. The total project budget is about \$1.7 million over 4 years, with about \$250K per year earmarked for IPST. A decision has been expected for some time, but there have been delays in awarding contracts for the Mill of the Future Solicitation.

2. Development of Materials for Service in Black Liquor Recovery Boilers

This proposal was originally prepared by Babcock and Wilcox , ORNL, IPST, Paprican and Weyerhaeuser. However, the requested funding levels could not be supported, so the program was scaled back, and total funding at the level of \$500K was received in 1995. The focus will be on cracking of composite tubes rather than the broader scope of the original proposal. IPST's subcontract will amount to \$120K for 1995. The program is expected to be complete in 4 years, and future funding levels are expected to be consistent with this year's.

The project will involve field evaluation of failed parts, investigation of environmental conditions responsible for cracking and corrosion, and laboratory testing of possible

cracking failure mechanisms. The approach will be to determine the state-of-the-art knowledge about cracking of composite tubes in recovery boilers by soliciting copies of any failure analysis reports, published and private. Visits to tube manufacturers and fabricators will also be made. In addition, temperature measurements and smelt samples will be taken in operating boilers. An Industrial Advisory Board has been established to interface with the project team.

CORROSION CONTROL IN CLOSED-CYCLE MILLS
PROJECT F019

ANNUAL RESEARCH REVIEW

March 23, 1995

Jeffery A. Colwell

Institute of Paper Science and Technology
500 10th Street, NW
Atlanta, GA 30318

TECHNICAL PROGRAM REVIEW

Project Title: CORROSION IN CLOSED CYCLE MILLS
Project Code: CCCMO
Project Number: F019
Division: Chemical and Biological Sciences
Project Staff: J. Colwell, G. Fonder
FY 94-95 Budget: \$ 47,000

Program Objective:

Identify key corrosion and materials issues which may impact the successful implementation of various closed mill scenarios and provide support to maximize the potential of these new technologies.

Summary of Results:

This project began on July 1, 1995. During the most recent PAC review on October 18, 1994, the complexity of this project was discussed at length. The original plan was to identify process changes in specific parts of the mill, quantify the chemistry and conditions in the environment which will impact materials of construction, and then publish a materials usability guideline document. It became clear from an initial review of the literature, and our discussions, that process design and engineering is still underway, and it may take some time before enough information is available to select materials for closed mills.

An alternative approach was proposed in which various materials limitations are to be summarized for future use by process engineers. The main departure from the original approach is that rather than working in parallel toward mill closure, we will be starting at the "end" of the process from a specific material's viewpoint and working in the reverse direction to meet designers in the middle. This will essentially involve setting limits for various materials in expected closed mill environments by defining a pathway and how far one might get down that pathway using a particular material. Alternatively, this work may also allow process engineers to identify where elemental purges would be required to maintain the use of a specific material.

To begin the process and develop the methodology, it was agreed at the PAC meeting that the bleach plant would be selected as the starting point. There are two reasons

for this; one, there have been many studies focused on bleach plant materials over the years and, two, bleach plant effluent reduction will continue to be a focal point of mill closure efforts in the next few years.

During a follow-up conference call on December 12 with PAC members, it became clear that there was a difference of opinion regarding priorities for this project. Several committee members believed that the best place to start would be the paper machine because of the potential for underdeposit corrosion. In addition, there was also some concern about chloride in recovery boilers being the most important issue. Consequently, we agreed to begin with the bleach plant and then move to other areas as quickly as possible.

In November, Jeff Colwell was asked by the Institute to serve as Acting Manager of the EPRI Pulp and Paper Office, which is operated under contract to EPRI. This left only limited time to commit to the project and progress since December has been very limited.

Goals for FY 1995-1996:

1. Restart the project and reach the milestones that were identified previously (Colwell).

VERTICAL TUBE FURNACE

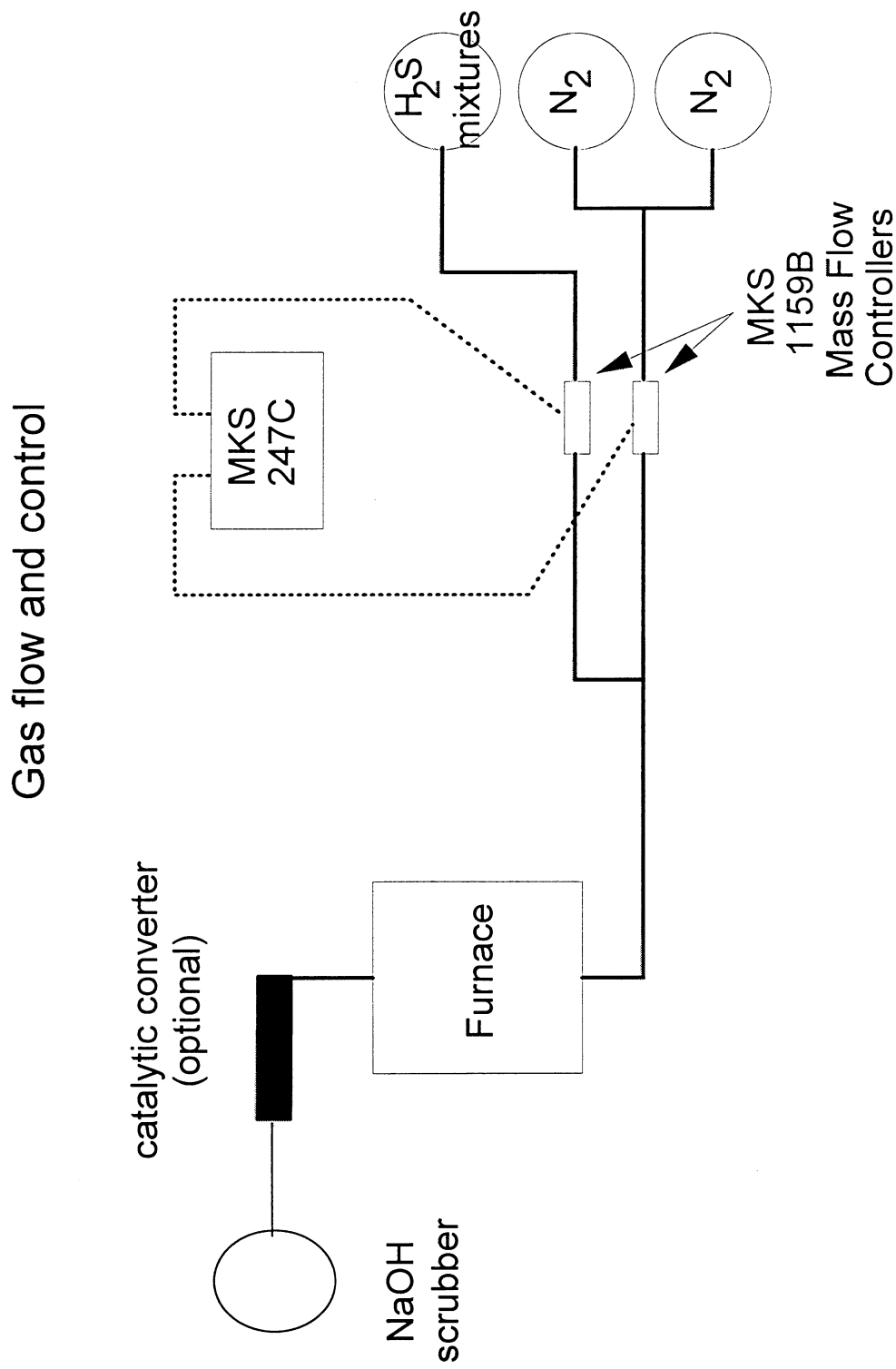


Figure 1. Schematic of the Experimental Arrangement.

FURNACE DETAILS

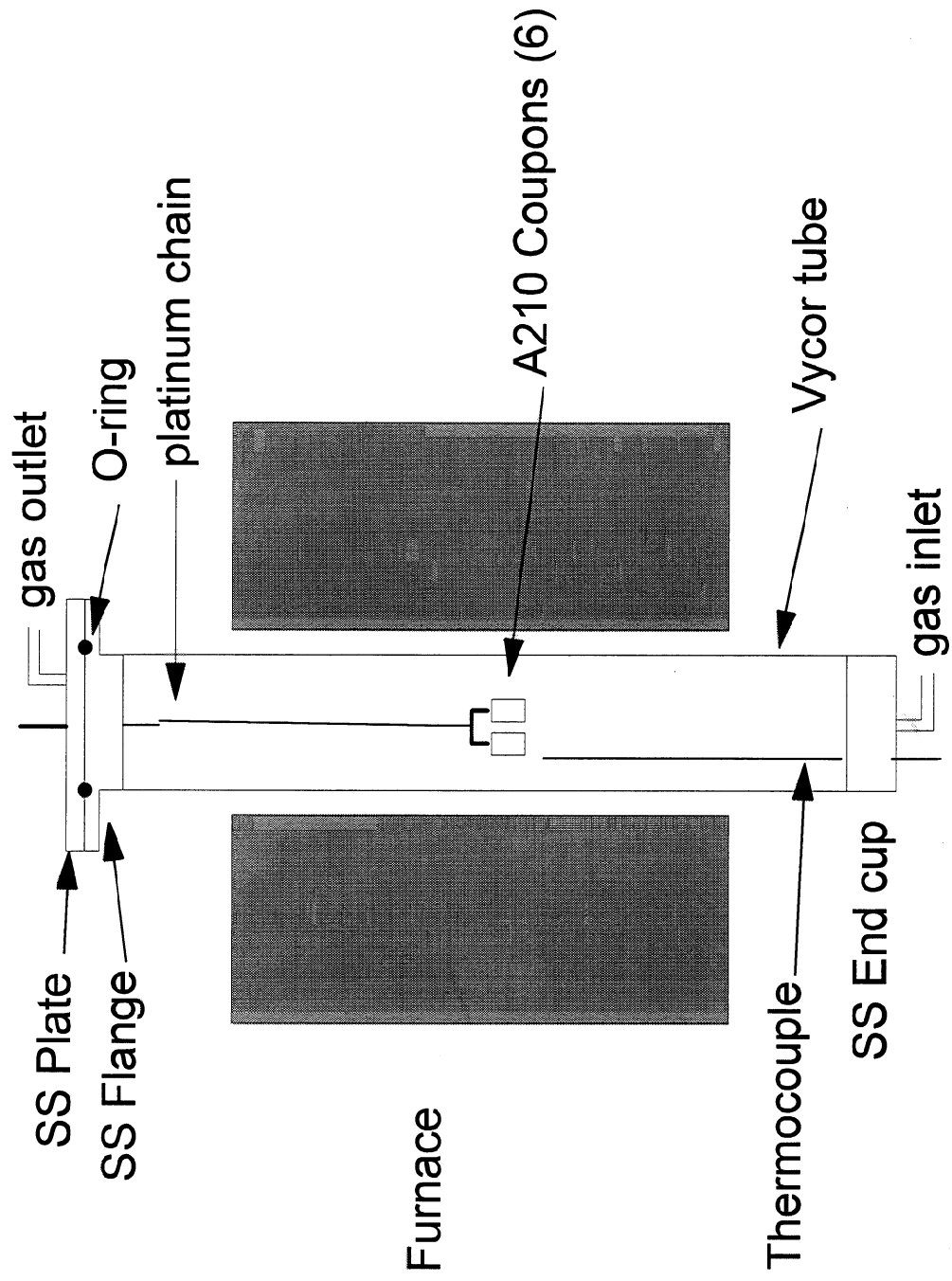


Figure 2. Schematic of Furnace Details.

H₂S/SO₂ Static Tests

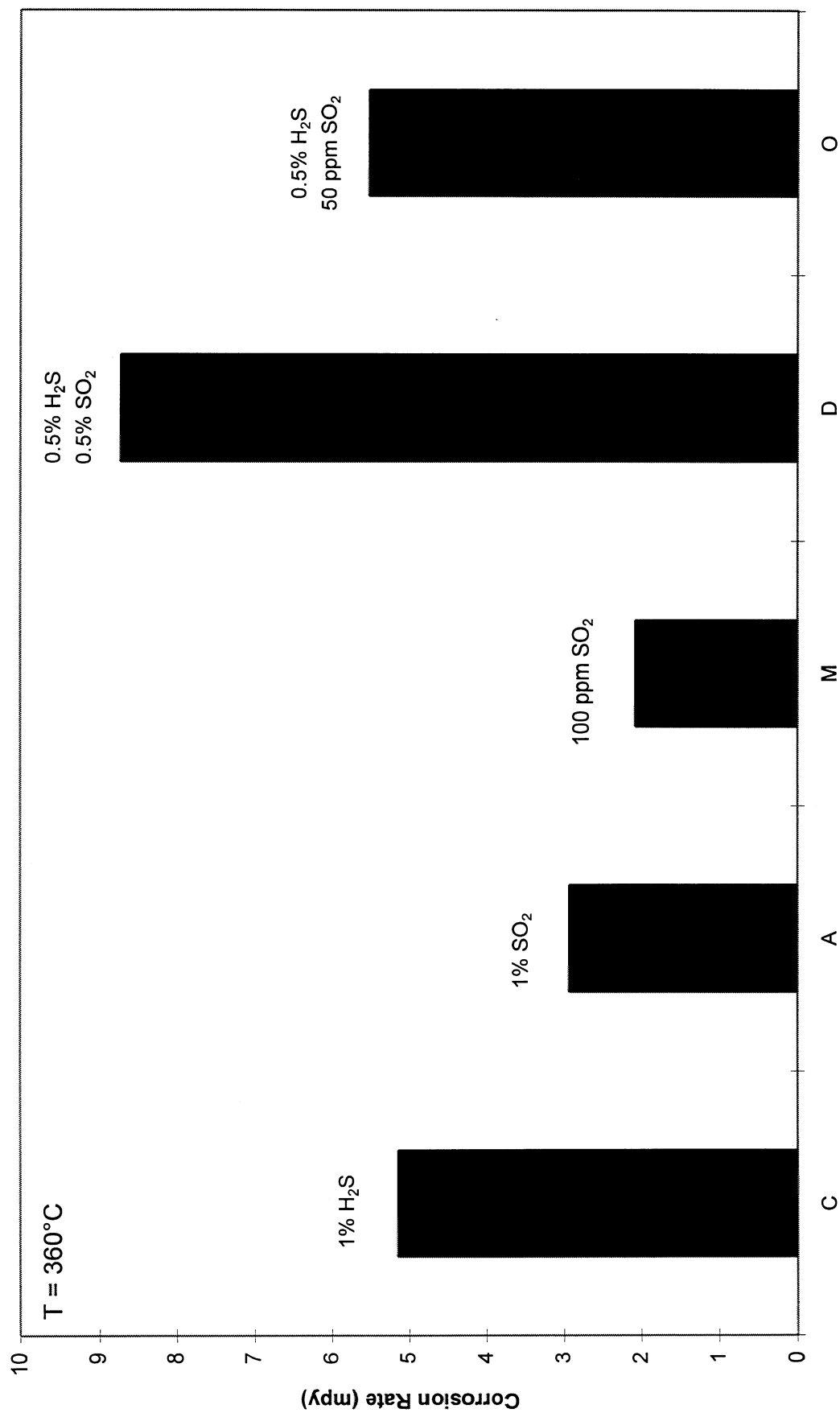


Figure 3. Corrosion Rate for Carbon Steel at 360°C under Constant Environmental Conditions.

H₂S/SO₂ Cyclic Tests

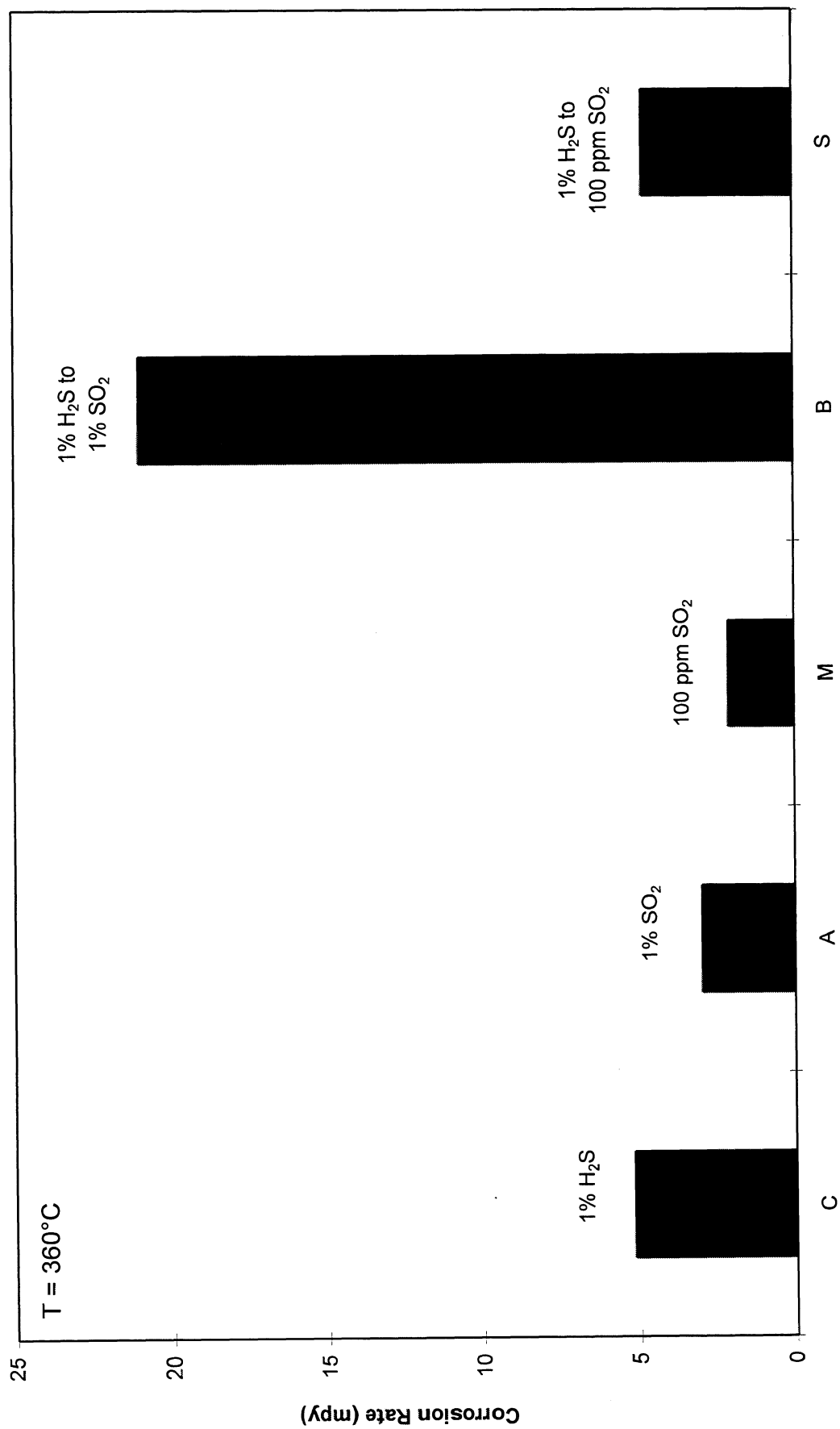


Figure 4. Corrosion Rates for Carbon Steel at 360°C Under Cyclic Environmental Conditions.

H₂S/SO₂ Pre-oxidation Tests

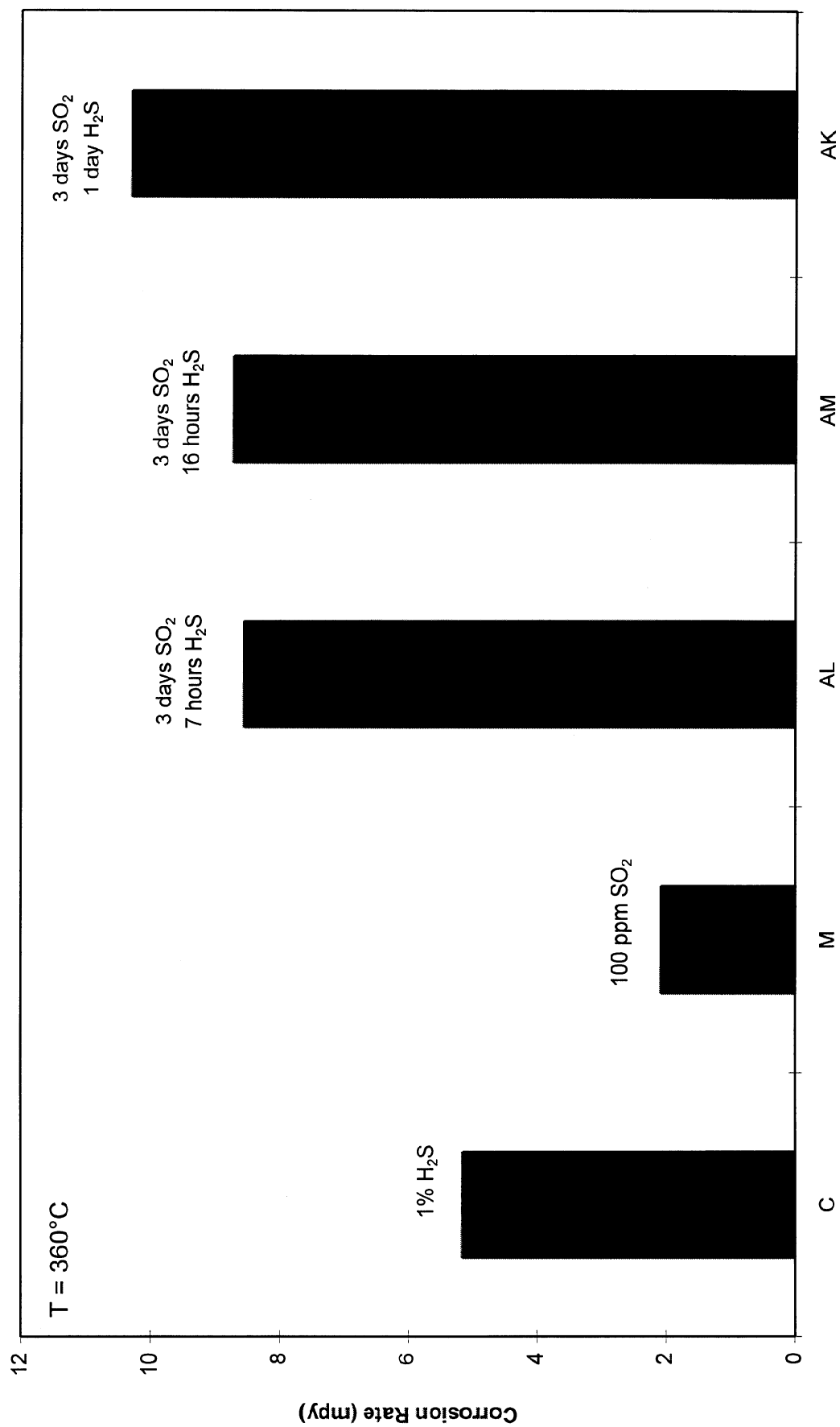


Figure 5. Results Showing Preoxidation of Carbon Steel in 100 ppm SO₂ at 360°C does not Stop Acceleration of Corrosion.

Quartz Spring Balance

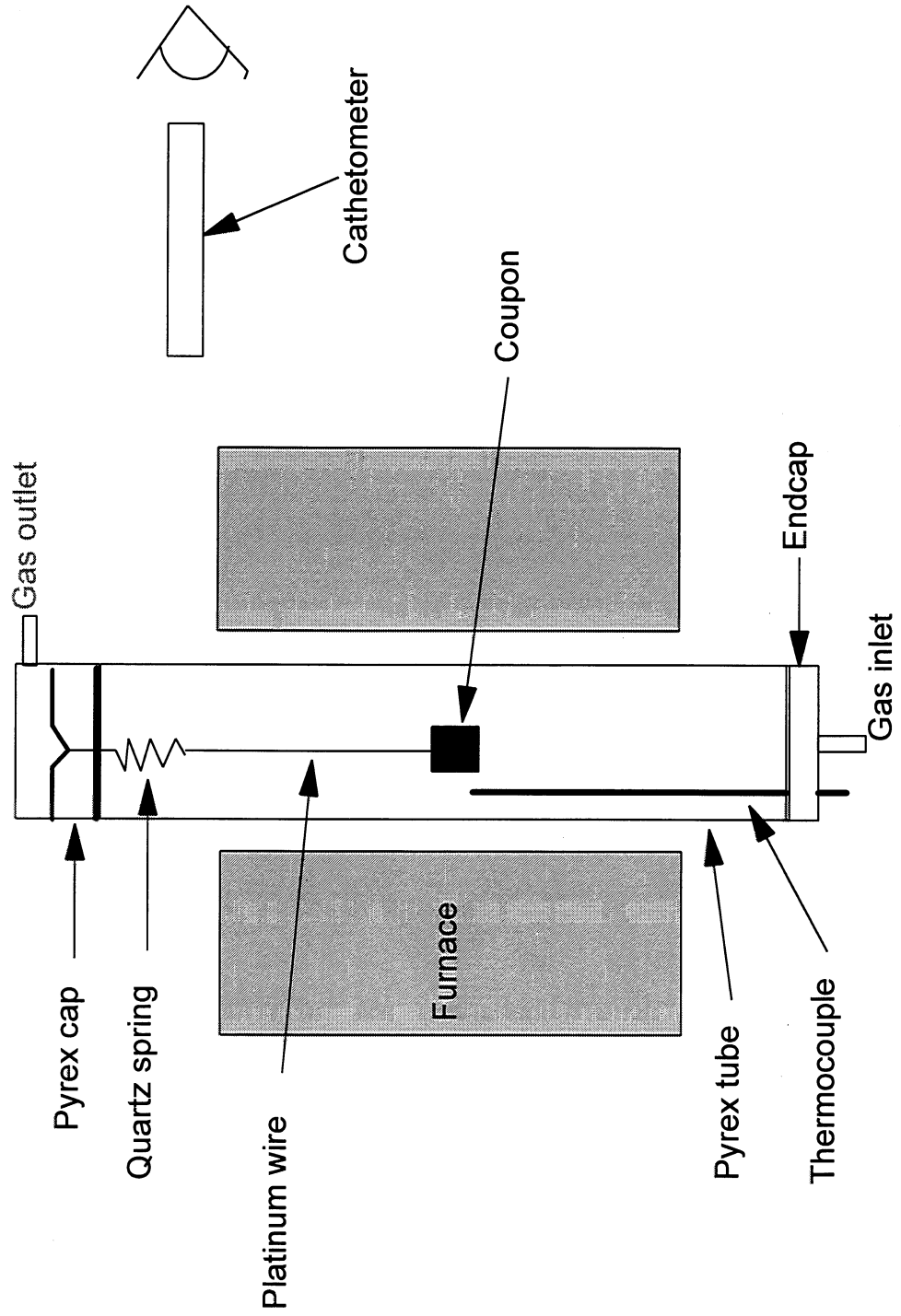


Figure 6. Schematic of the Quartz Spring Balance.

Carbon Steel Coupons in Alternating 1% SO₂ and 1% H₂S Environment

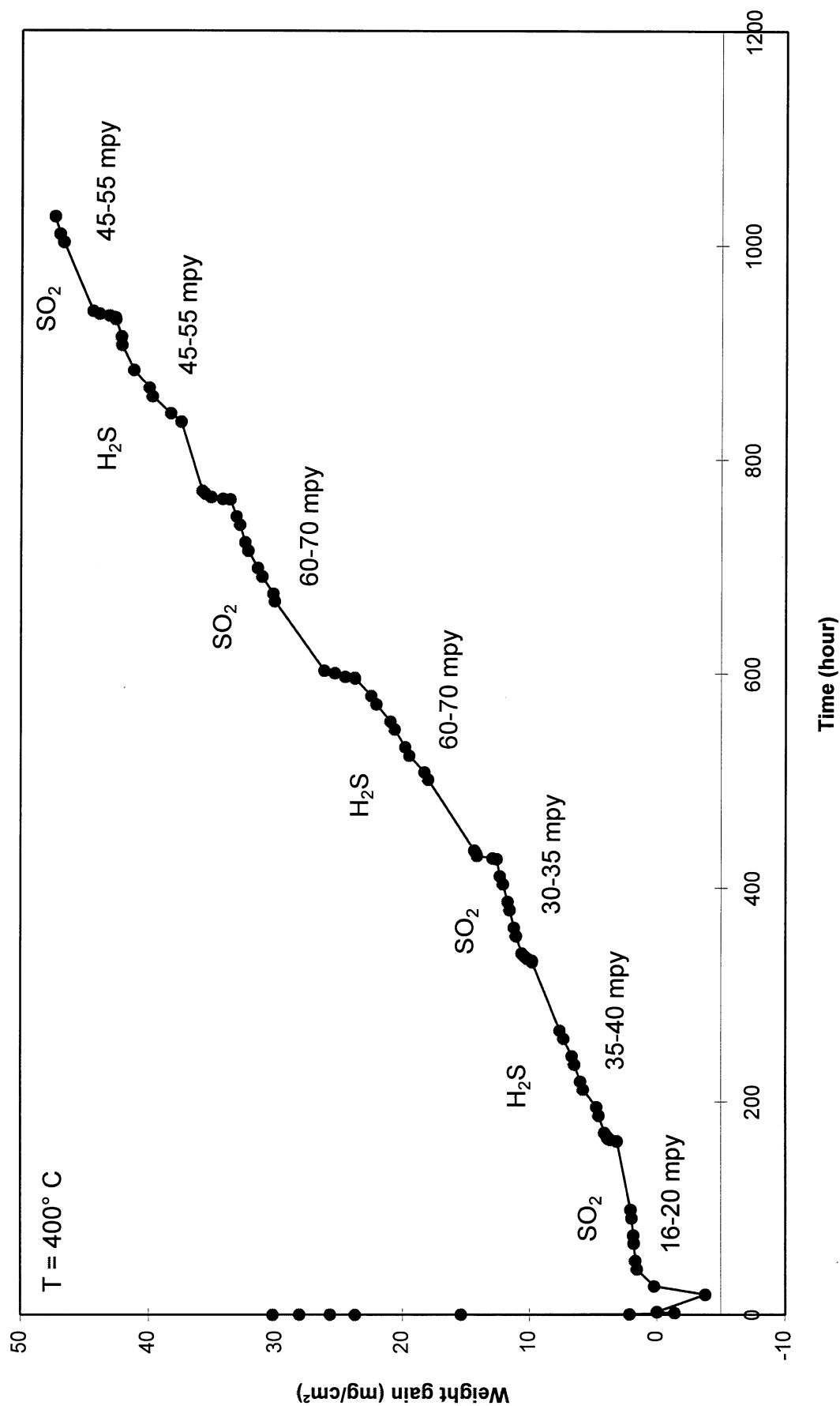


Figure 7. Weight Gain vs. Time for Cyclic Tests of Carbon Steel at 400°C.

Carbon Steel Coupon in 1% H₂S Environment

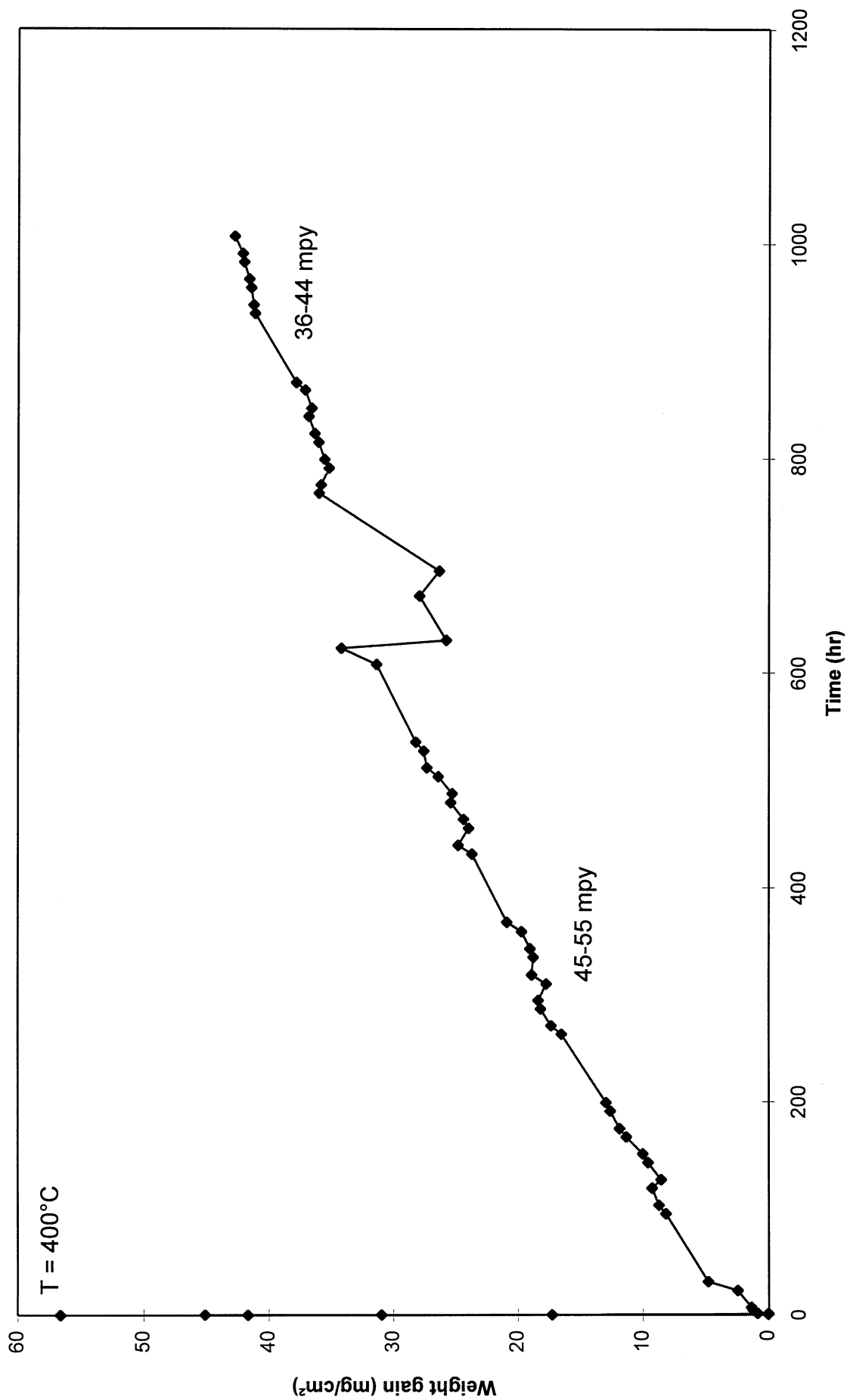


Figure 8. Weight Gain vs. Time for Carbon Steel in 1% H₂S at 400°C.

Spec. #	Temp., °C	Time, hr	Wt. Gain, g/cm ² x10 ⁻⁴	MPY	Wt. Loss, g/cm ² x10 ⁻⁴	MPY
227			21.67	10		
336		312	17.40	4	37.31	9
337			33.66	8	57.30	13
300	440	4	3.34	61	5.21	95
301			3.81	70		
303		8	5.11	47	9.48	87
306			5.27	48		
220		24	5.88	18	9.45	29
221			5.95	18		
222		72	6.98	7		
223			6.66	7	13.48	14
304		4	3.91	72	6.80	124
309			4.88	90		
302		8	7.68	70		
311			9.31	85	17.73	163
329	480	24	6.75	20		
335			14.10	43	15.09	46
331		72	13.24	14	44.12	45
332			6.35	7	46.98	47

Comparison of Cyclic and Baseline Test for Carbon Steel Coupons

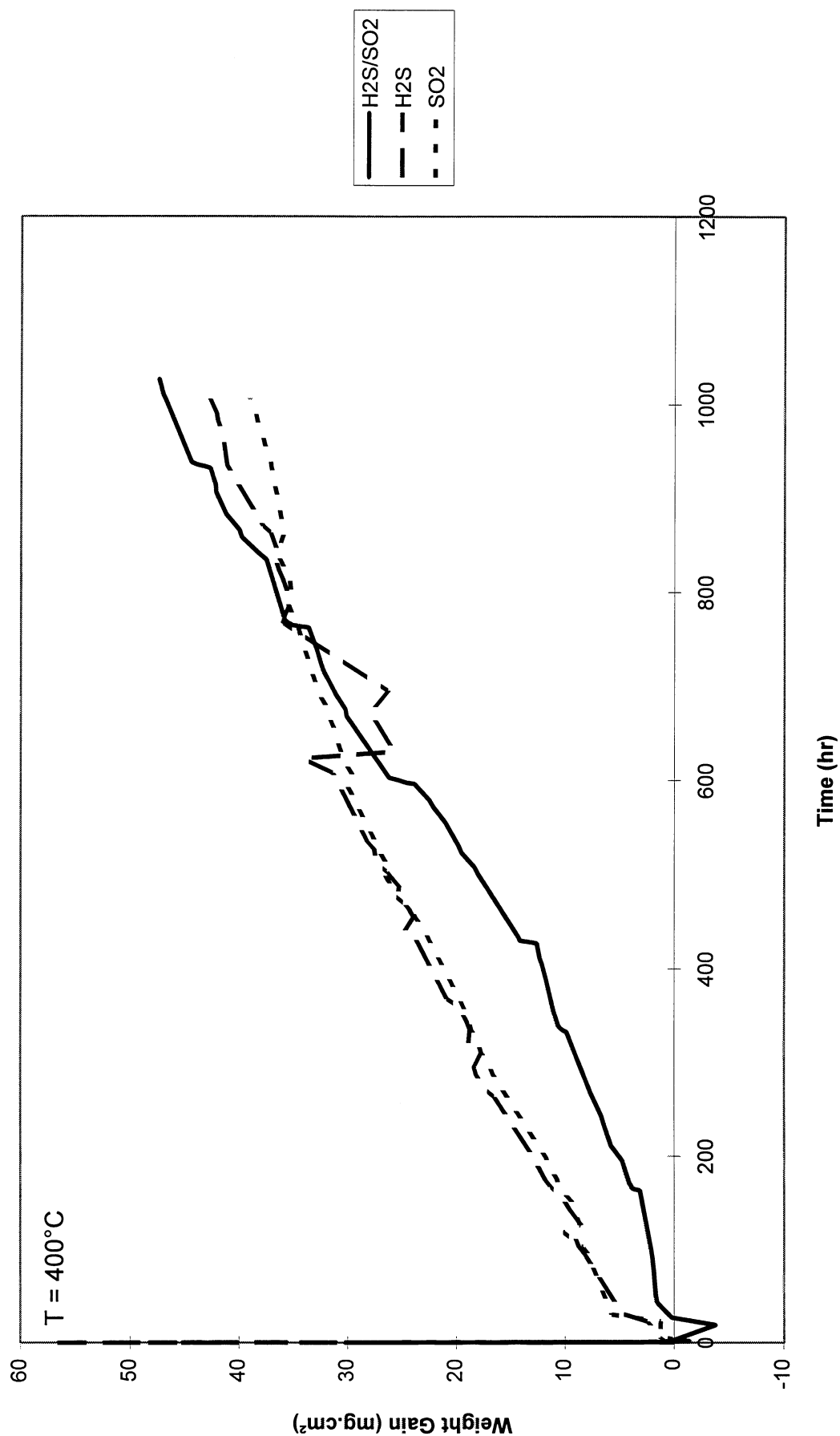


Figure 10. Comparison of Curves from Figures 7, 8, and 9.

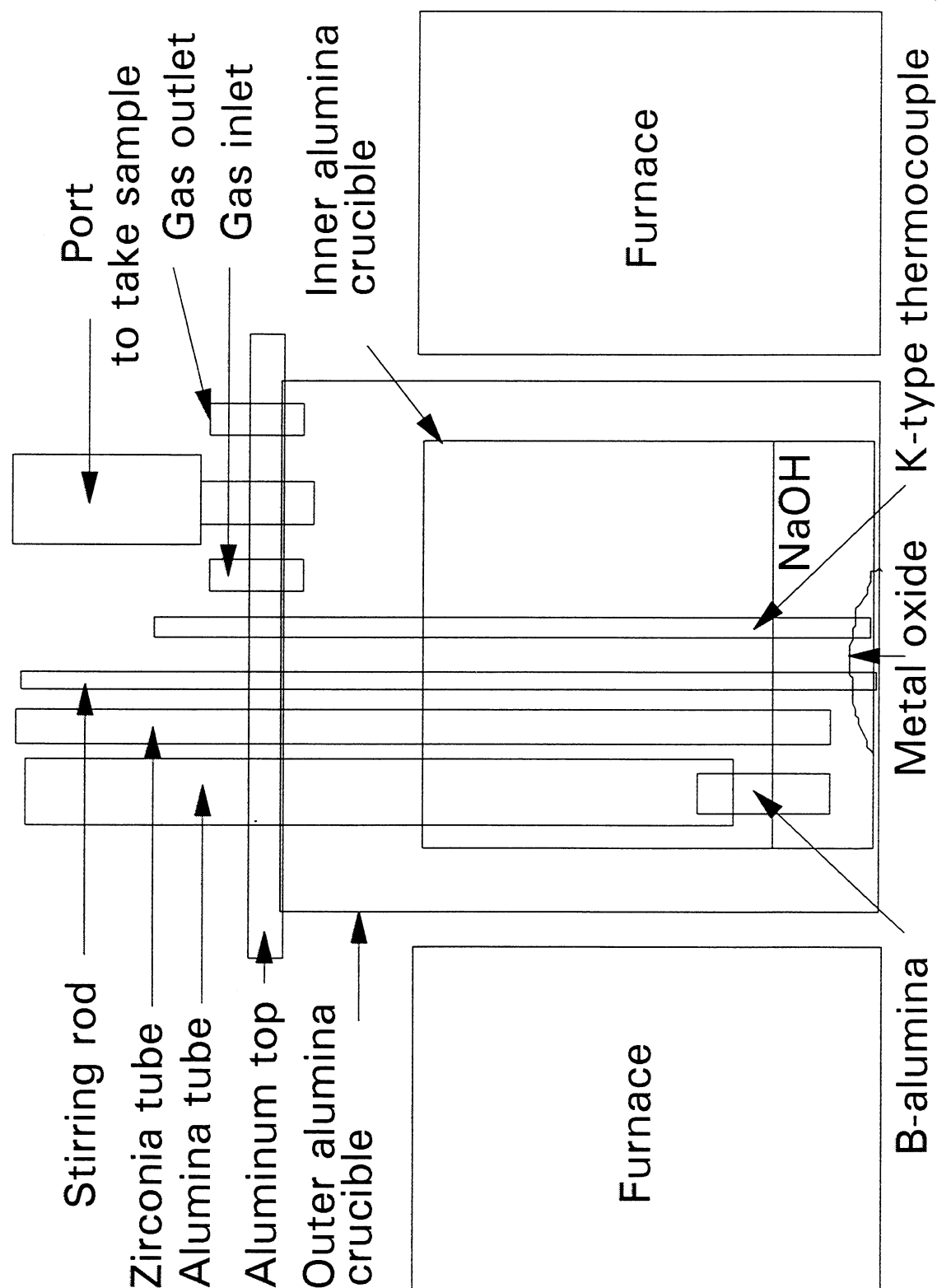


Figure 11. Experimental Set Up for Basicity and Solubility Measurements in Molten Hydroxide.

Thermodynamic diagram of Cr in NaOH at 350 C

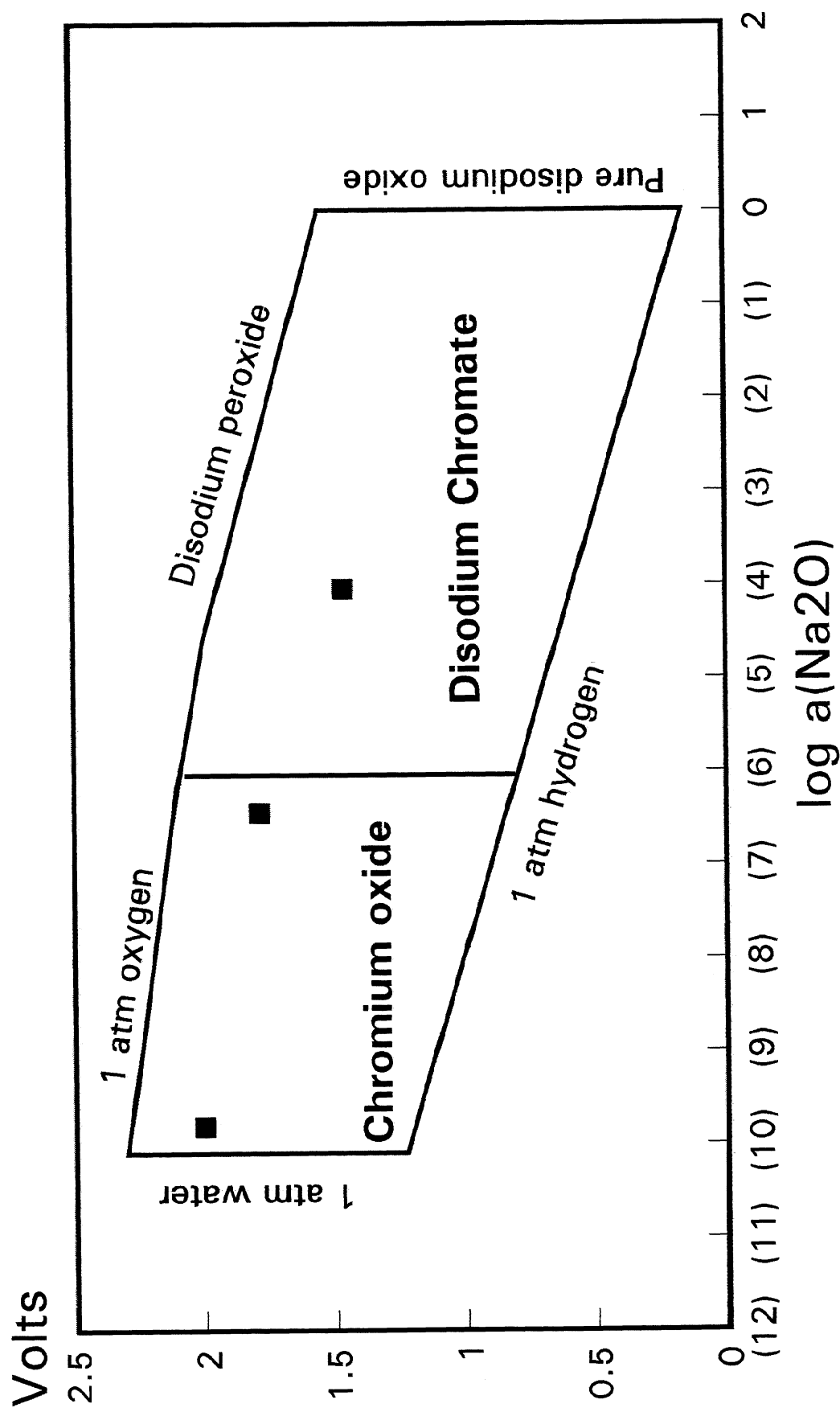


Figure 12. Phase Stabilities in Na-Cr-O-H System at 350°C. Three experimental basicities are Shown on the Diagram.

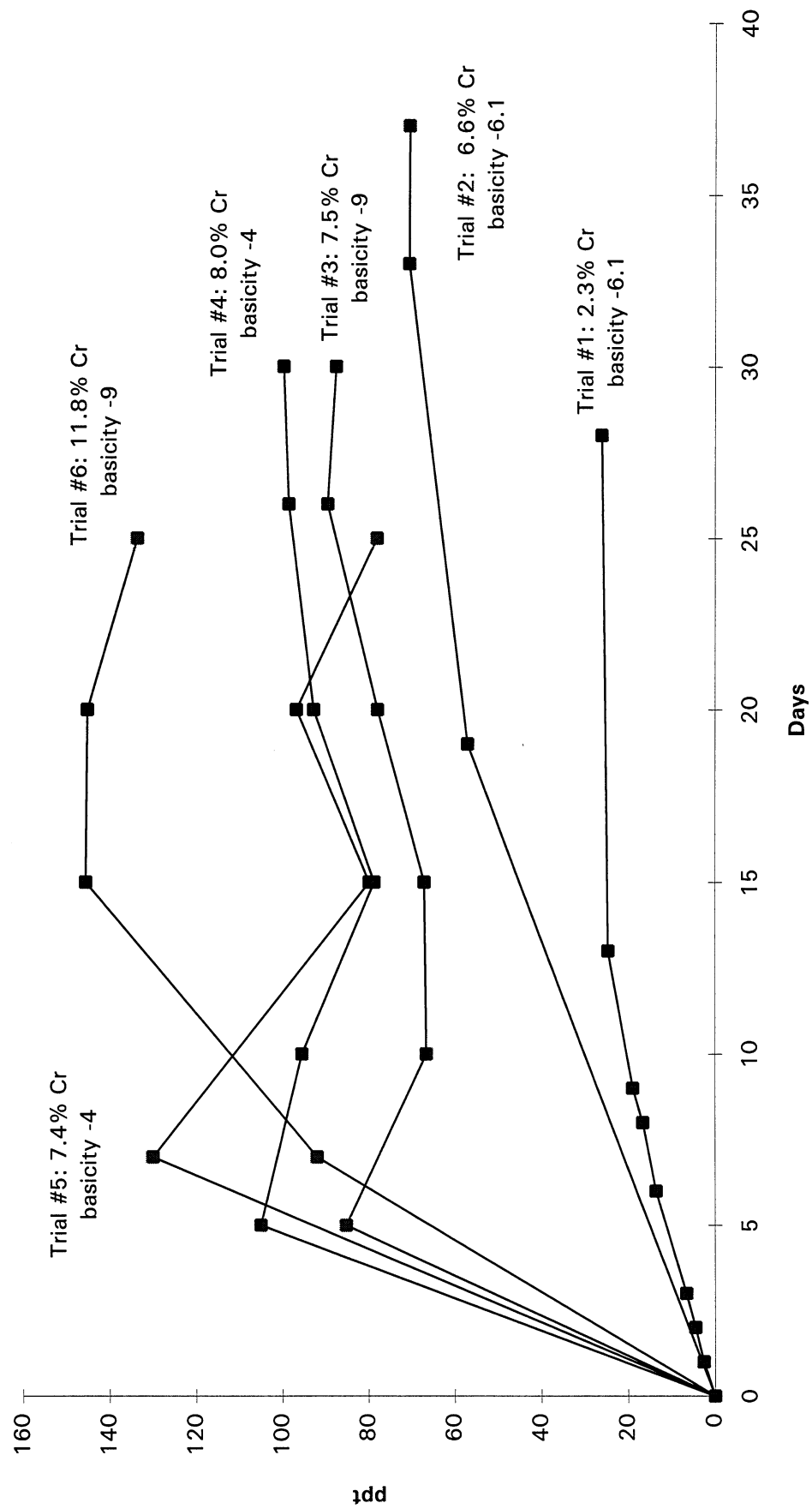


Figure 13. Cr Concentration vs. Time for Different Basicities.

Galvanic Current between Carbon Steel and Stainless Steel in Molten Smelt @ 800° C

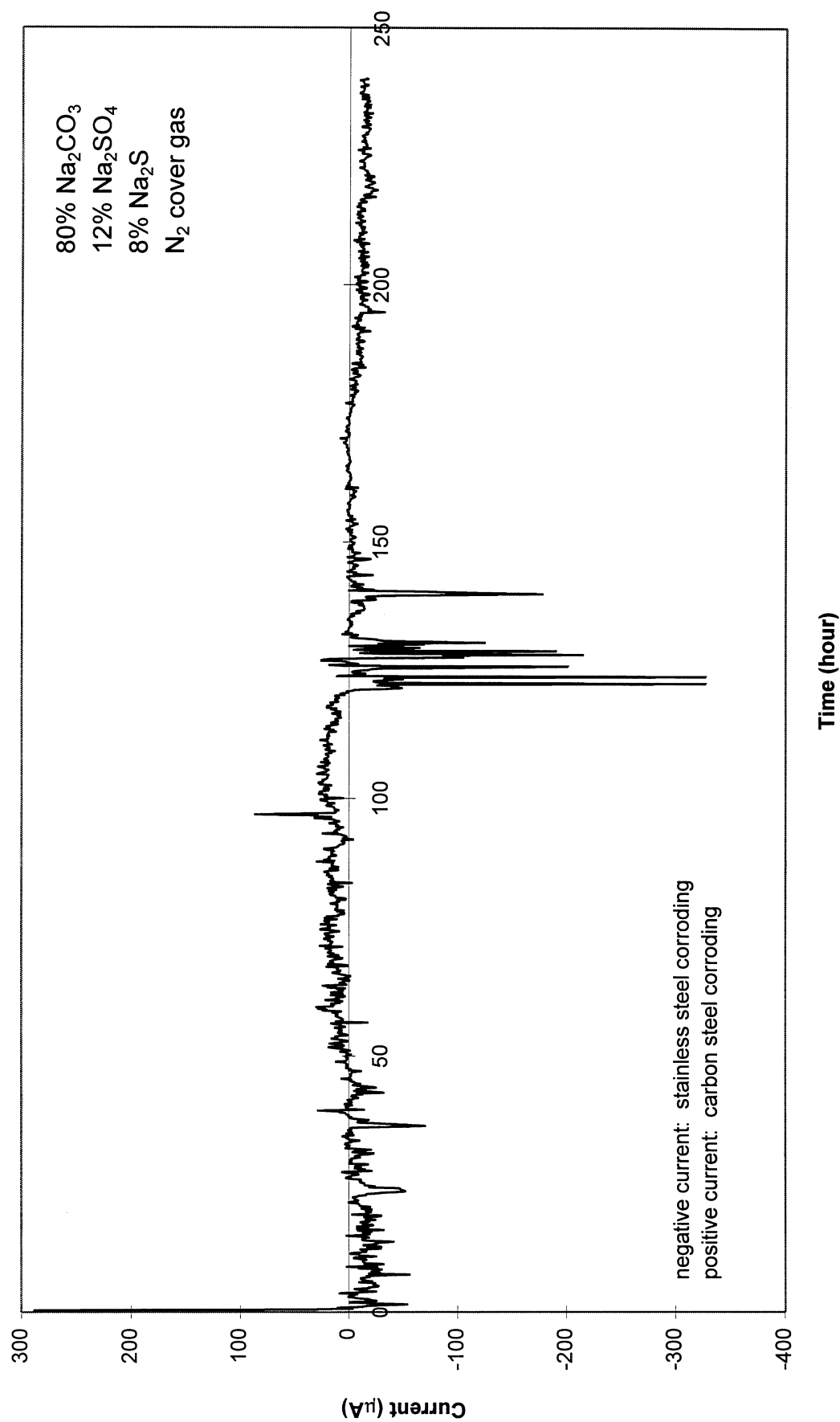


Figure 14. Current vs. Time for Carbon Steel Coupled to Stainless Steel in Molten Smelt at 800°C.



Figure 15. Photograph of the Carbon Steel and Stainless Steel wire samples at the end of the galvanic test.

Galvanic Current between Carbon Steel and Stainless Steel in Molten Smelt @ 800°C

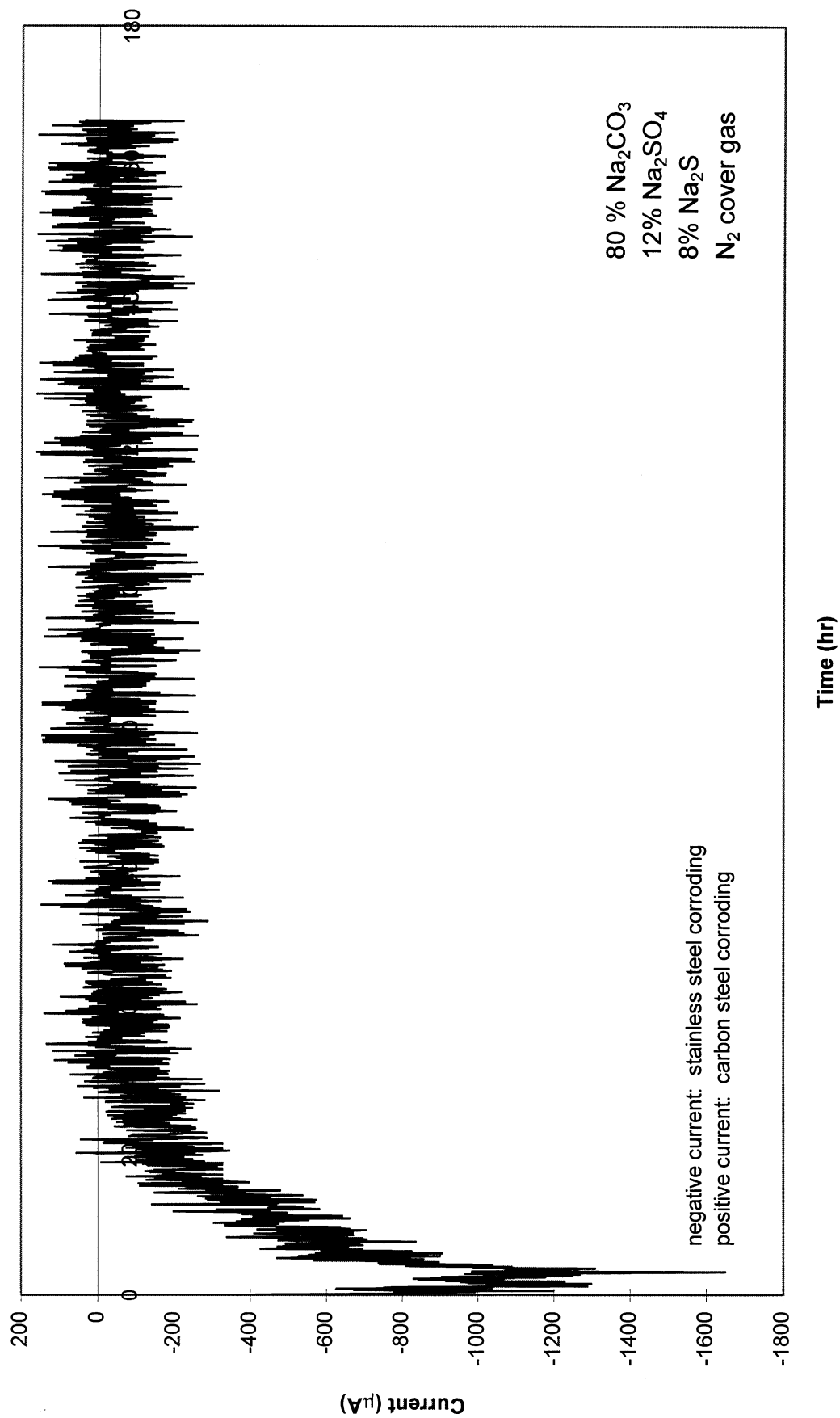


Figure 16. Current vs. Time Curve for Galvanic Measurements.

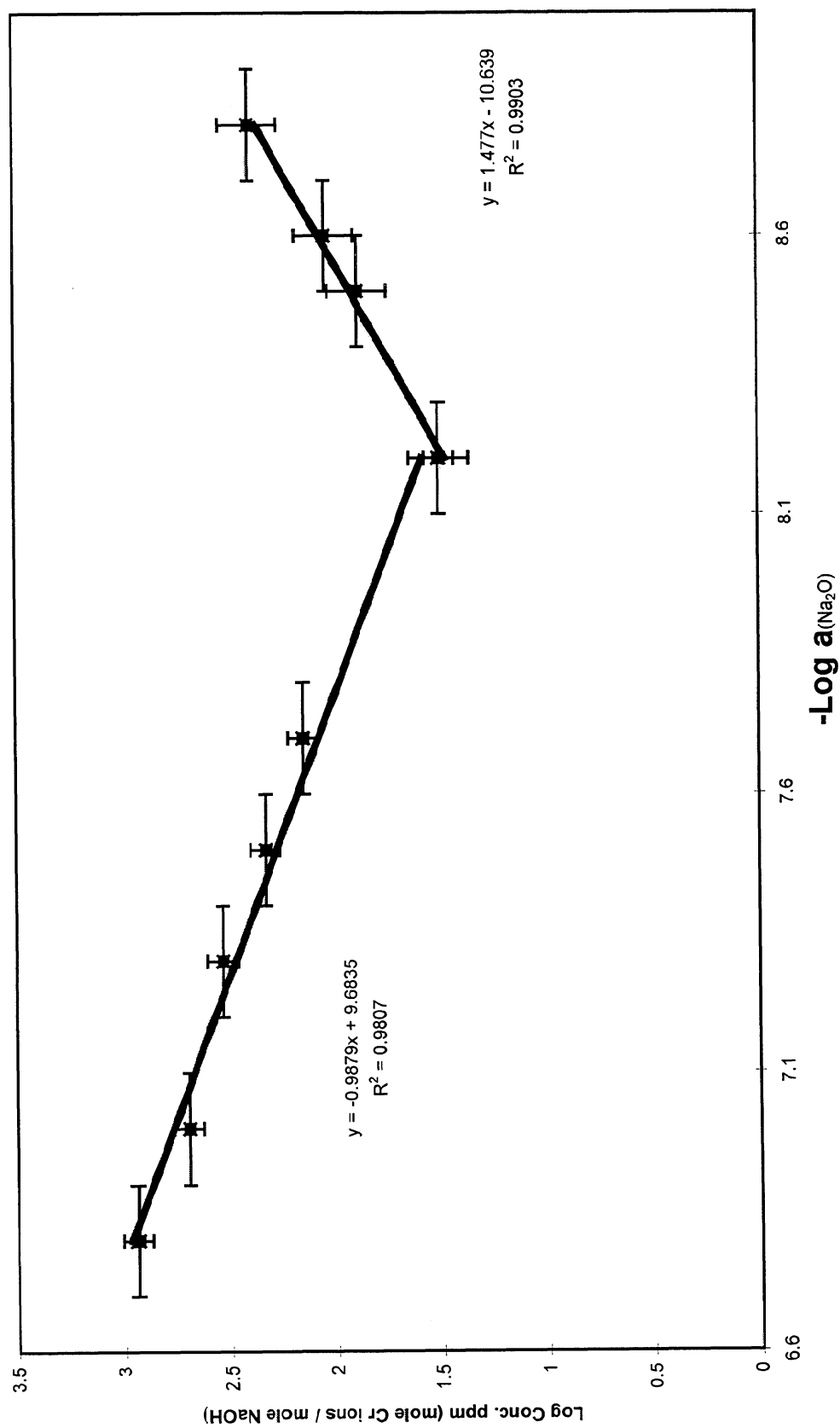


Figure 9. Solubility of Cr_2O_3 in NaOH.

Galvanic Current between Carbon Steel and Stainless Steel in Molten Smelt @ 800°C

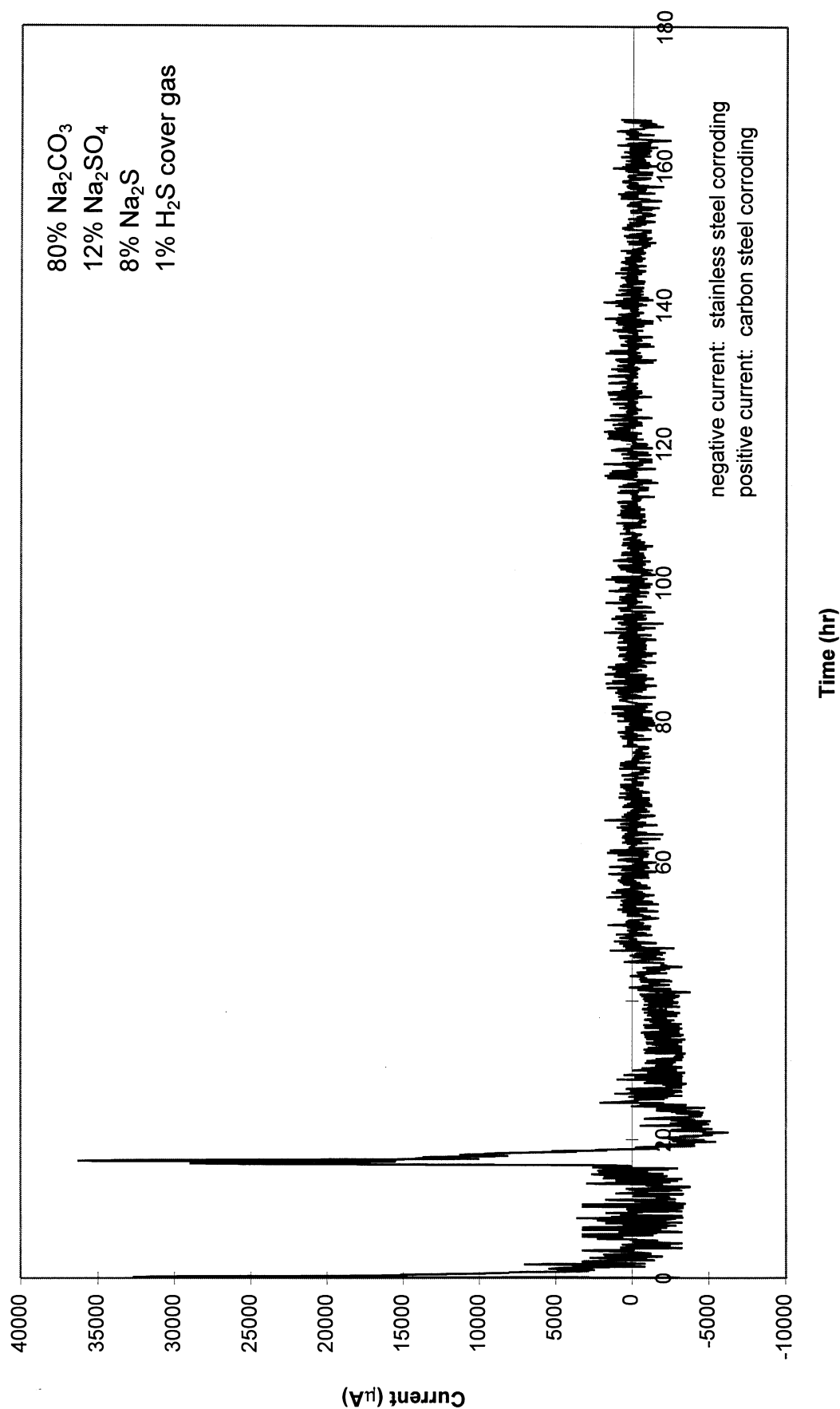


Figure 18. Current vs. Time Curve for Galvanic Measurements.

Carbon Steel Coupon in 1% SO₂ Environment

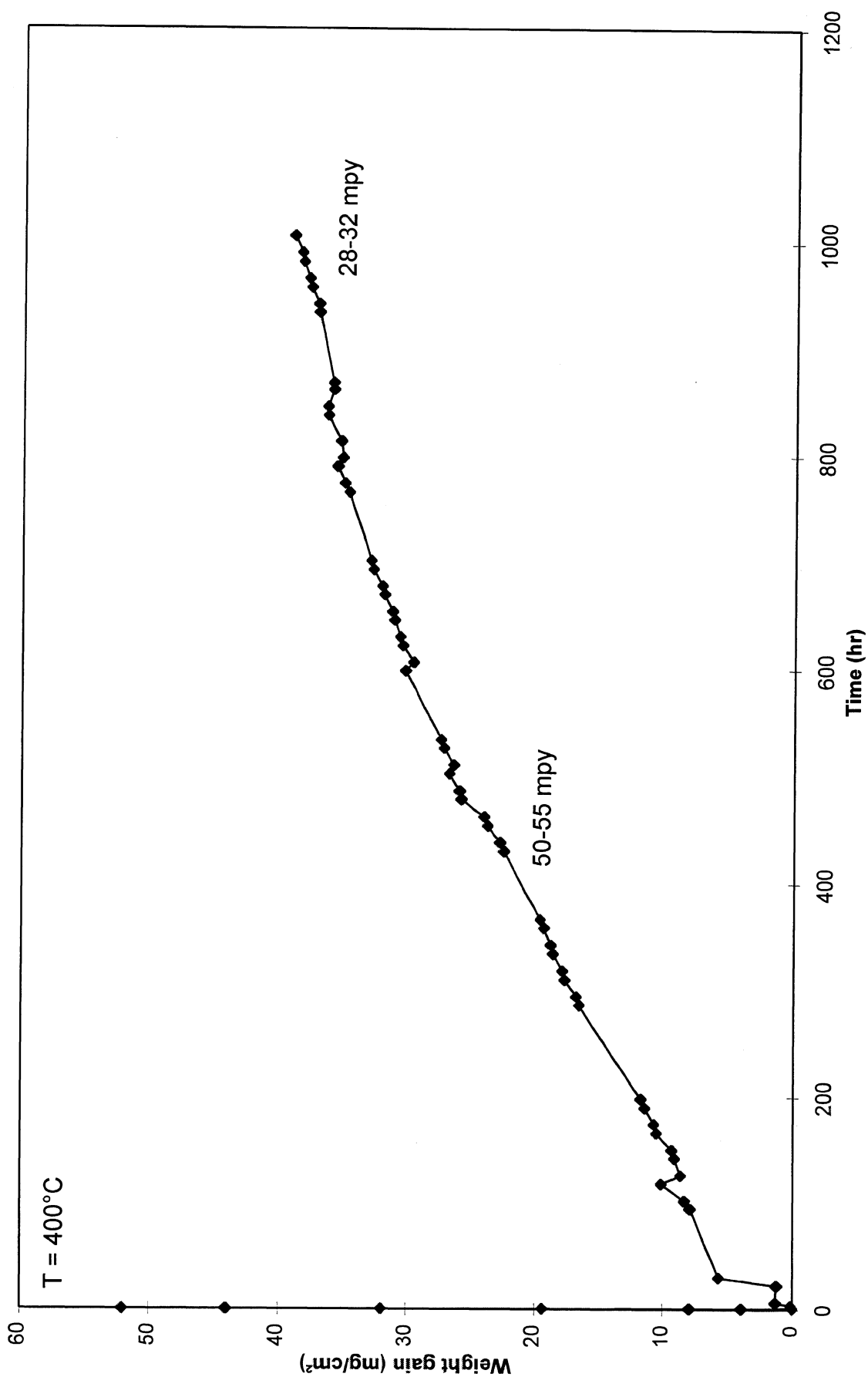


Figure 9. Weight Gain vs. Time for Carbon Steel in 1% SO₂ of 400°C.

